

**SERIES RESONANT SWITCHED CAPACITOR CONVERTER FOR  
ELECTRIC VEHICLE LITHIUM-ION BATTERY CELL VOLTAGE  
EQUALIZATION**

**ALI AHMED**

A Thesis

in

The Department

of

Electrical and Computer Engineering

Presented in Partial Fulfillment of the Requirements for the

Degree of Master of Applied Science (Electrical Engineering and Computer Science) at

Concordia University

Montréal, Québec, Canada

September 2012

© ALI AHMED, 2012

**CONCORDIA UNIVERSITY  
SCHOOL OF GRADUATE STUDIES**

This is to certify that the thesis prepared

By:           Ali Ahmed

Entitled:     “Series Resonant Switched Capacitor Converter for Electric Vehicles  
Lithium-Ion Battery Cell Voltage Equalization”

and submitted in partial fulfillment of the requirements for the degree of

**Master of Applied Science**

Complies with the regulations of this University and meets the accepted standards with respect to originality and quality.

Signed by the final examining committee:

\_\_\_\_\_ Chair  
Dr. S. Abdi

\_\_\_\_\_ Examiner, External  
Dr. A. Bagchi, BCEE To the Program

\_\_\_\_\_ Examiner  
Dr. L. A. Lopes

\_\_\_\_\_ Supervisor  
Dr. S. Williamson

Approved by: \_\_\_\_\_  
Dr. W. E. Lynch, Chair  
Department of Electrical and Computer Engineering

\_\_\_\_\_20\_\_\_\_\_

\_\_\_\_\_ Dr. Robin A. L. Drew  
Dean, Faculty of Engineering and  
Computer Science

# **ABSTRACT**

## **Series Resonant Switched Capacitor Converter for Electric Vehicles Lithium-Ion Battery Cell Equalization**

**Ali Ahmed**

Extending the lifetime of the battery system of the Electric Vehicles will affect the economic feasibility of the vehicle. Connecting the battery cells in series raise the problem of imbalance voltages of the cells caused by Difference of internal resistance, imbalanced SoC, gradients of ambient temperature of the battery pack during charging and discharging.

The commercial solution for this problem is shunting the cell with extra charge to a dissipative resistor and gets rid of the extra charge as heat.

This thesis proposes the use of Serial Resonant Switched Capacitor Converter for battery Cell Voltage equalization, which allows the extra charge to be transferred to other cell instead of dissipated it as heat. The thesis can be divided into five parts: the first part is introduction to the lithium-ion battery system, estimation of the State of Charge and battery modeling; the second part is a review for the switching topologies that used for battery cell equalization; the third part is the modes of operation of the proposed converter, modeling and simulation. And also introducing the new concept of controlled switching which allow the use of current sharing technique to reduce the equalization time. The fourth part is building the prototype circuit and allows the microcontroller to tune the circuit to achieve the zero current switching and the last part is the conclusion and the future work

## **ACKNOWLEDGMENTS**

The author would like to express his most sincere gratitude to his supervisor, Dr. Sheldon S. Williamson, for his patient and invaluable guidance, advice, and friendship throughout the Master's program.

The author also would like to extend a special vote of gratitude towards Prof. Louis Lopes, for his valuable suggestions and comments.

To my role model my father, to my mother which without her praying for  
me I can't reach this step

To my patient and supportive wife

# TABLE OF CONTENTS

<b>LIST OF FIGURES .....</b>	<b>viii</b>
<b>LIST OF ACRONYMS .....</b>	<b>xi</b>
<b>LIST OF PRINCIPAL SYMBOLS .....</b>	<b>xii</b>
<b>CHAPTER 1 .....</b>	<b>1</b>
INTRODUCTION .....	1
1.1 INTRODUCTION .....	1
1.2 BATTERY MANAGEMENT SYSTEM .....	2
1.3 SOC ESTIMATION. ....	2
1.4 BATTERY MODELING .....	3
1.4.1 RUN-TIME BATTERY MODEL .....	4
1.4.2 GENERIC BATTERY MODEL .....	5
1.5 CONTRIBUTION OF THE THESIS .....	6
1.6 THESIS OUTLINE .....	6
<b>CHAPTER 2 .....</b>	<b>8</b>
<b>REVIEW OF SWITCHED CONVERTER TOPOLOGIES FOR ELECTRIC VEHICLE BATTERY</b>	
<b>CELL EQUALIZATION .....</b>	<b>8</b>
2.1 INTRODUCTION .....	8
2.2 MODIFIED CUK CONVERTER .....	11
2.3 BUCK-BOOST AND QUASI-RESONANT ZERO CURRENT BATTERY EQUALIZING .....	14
2.4 FLY-BACK EQUALIZER AND THE MODULARIZED TECHNIQUE .....	20

2.5	THE SWITCHED CAPACITOR BATTERY EQUALIZING TOPOLOGY....	23
2.6	SUMMARY .....	25
CHAPTER 3 .....		26
THE PROPOSED SERIAL RESONANT SWITCHING CAPACITOR CONVERTER .....		26
3.1	INTRODUCTION .....	26
3.2	MODES OF OPERATION .....	29
3.3	MATHEMATICAL MODELING .....	31
3.4	CIRCUIT DESIGN AND SIMULATION .....	34
3.4.1	CONTROLLED SWITCHING AND CURRENT SHARING .....	36
3.4.2	EQUALIZATION TIME .....	43
3.5	SUMMARY .....	44
CHAPTER 4 .....		46
EXPERIMENTAL SETUP AND TEST RESULTS.....		46
4.1	INTRODUCTION .....	46
4.2	CONTROL CIRCUIT AND TUNING .....	47
4.3	CONTROLLED SWITCHING AND EQUALIZATION TIME .....	50
4.4	SUMMARY .....	55
CHAPTER 5 .....		56
CONCLUSIONS AND FUTURE WORK .....		56
5.1	SUMMARY .....	56
5.2	FUTURE WORK .....	58
REFERENCES .....		60

# LIST OF FIGURES

Fig. 1-1 Kalman filter method for SoC estimation-----	3
Fig. 1-2 Run-time battery model-----	4
Fig. 1-3 Generic battery Model -----	5
Fig 2-1 Balance Battery Cells -----	8
Fig. 2-2 imbalance Battery Cells -----	9
Fig. 2-3 dissipative method commercially used in Vehicles -----	10
Fig2-4 individual cell equalization method-----	11
Fig. 2-5 the proposed battery equalizer using modified CUK converter. -----	12
Fig.2-6 Q1 is turned ON-----	12
Fig. 2-7 Q1 is turned OFF-----	13
Fig. 2-8 Buck-Boost Battery equalizer -----	15
Fig. 2-9 Buck-boost QRZCS battery equalizer circuit-----	15
Fig.2-10 the Modified QRZCS Battery equalizer -----	16
Fig.2-11 the equivalent circuit and switching waveform -----	16
Fig 2-12 QRZCS Period $t_0 < t < t_1$ -----	17
Fig.2-13 QRZCS the Period $t_1 < t < t_2$ -----	18
Fig.2-14 QRZCS the Period $t_2 < t < t_3$ -----	18
Fig.2-15 QRZCS Period $t_3 < t < t_4$ -----	19
Fig.2-16 proposed fly-back equalizer-----	20
Fig.2-17 proposed modularized charge equalizer circuit consist with M=2 and N=2equalizer ---	21
Fig.2-18 Fly-Back equivalent circuit of period $t_0 < t < t_1$ -----	22
Fig.2-19 SCC for battery cell voltage equalization -----	24
Fig.2-20 two complimentary PWM signal with Duty cycle = 50%-----	25
Fig3-1 Resonance Switched Capacitor battery cell equalization Circuit -----	27



Fig.3-3 The power loss of the MOSFETs in ZCS -----	28
Fig.3-4 is showing simulation results of the current and the voltage of the MOSFET when the Gate signal is applied -----	28
Fig.3-4 MOSFET waveforms -----	29
Fig.3-5 State A charging the transfer elements -----	30
Fig.3-6 State B discharging the energy transfer elements to the battery cell-----	30
Fig.3-8 zero current switching when $F_{sw} = F_r$ -----	36
Fig 3-9 chaining equalization control-----	37
Fig 3-10 four cell SRSCC equalization-----	38
Fig 3-11 the proposed algorithm for equalization -----	39
Fig.3-12 State A of current sharing switching method -----	40
Fig.3-13 State B of current sharing switching method -----	41
Fig.3-14 B2 equalization current of the conventional method -----	42
Fig.3-15 B2 equalization current of the current sharing method -----	42
Fig.3-16 voltage equalization trajectory for conventional method(time in sec) -----	43
Fig.3-17 voltage equalization trajectory for current sharing method (time in sec) -----	44
Fig.4-1 the prototype board for the four cell battery equalization using SRSCC -----	47
Fig.4-2 Control circuit diagram -----	48
Fig.4-3 steps of tuning -----	49
Fig.4-4 Before tuning Waveforms-----	49
Fig.4-5 after tuning Waveforms -----	50
Fig.4-6 equalization current of B2 in SRSCC conventional method -----	51
Fig.4-7 equalization current of B2 current sharing method -----	52
Fig.4-8 the equalization time for two battery cell in SRSCC conventional method time in minutes -----	53
Fig.4-9 the equalization time for three battery cell in current sharing method ( in minutes) -----	54

# LIST OF ACRONYMS

BMS	Battery Management System
EMI	Electro-Magnetic Interference
ESR	Equivalent Series Resistance
EV	Electric Vehicle
ICE	Indi visual Cell Equalization
MOSFET	Metal Oxide Semiconductor Field Effect Transistor
OCV	Open Circuit Voltage
PHEV	Plug-in Hybrid Electric Vehicle
QRZCS	Quasi Resonant Zero Current Switching
SCC	Switched Capacitor Converter
SOC	State of Charge
SOH	State of Health
SRSCC	Serial Resonance Switched Capacitor Converter
ZCS	Zero Current Switching

# LIST OF PRINCIPAL SYMBOLS

A, B, C, D	State Space Constants
C	Capacitor
D	Duty cycle
$f_r$	Resonance Frequency
$f_{sw}$	Switching Frequency
L	Inductance
RDS-on	MOSFETs Drain to Source Resistance when ON

# CHAPTER 1

## INTRODUCTION

### 1.1 INTRODUCTION

It is not secret that the role of the batteries in our lives has evolved and became more and more important either through the widespread of the portable equipment and the need of them to last longer or through the need of less fuel consume cars by using electric cars or by using the plug-in hybrid electric vehicle (PHEV) due to the continue rising in the oil prices or simply for choosing to live green.

One of main batteries types that are used these days is the lithium-ion battery, due to their specification as non- memory effect , high working cell voltage, low environmental pollution, low self-discharge rate , and high power density in volume and high specific energy and energy density [1]. The density of power rate for a lithium-ion battery is triple that for a lead –acid battery, one and a half that of alkaline ones [1].

Due to the fact that the voltage in a single battery cell is inherently low, battery cells are usually connect in parallel to get higher current and in series to get higher voltages, the number of series and parallel branches depend on the type of application that are used in. normally in vehicles battery system about 100 cells are connected in series to produce 360 V for the alimentation of the system.

## **1.2 BATTERY MANAGEMENT SYSTEM**

Because of the nature of the lithium-ion batteries they need special attention to ensure they work safely, to do so every lithium-ion battery system must have a BMS, whether the battery cells is in laptop or in Electric Vehicle EV.

Monitoring the temperature of each cell of the battery, estimation of the SoC (State of Charge) and SoH (State of Health) for each cell and whole system, preventing the overcharging to eliminate the danger of explosion, preventing the over-discharging to eliminate permanent damage to the cell and battery cell equalization all those are the tasks of the BMS.

The scope of this thesis is the battery equalization problem and proposing a method to equalize the charge in the cells to prolong the lifetime of the battery and as a result prolong the lifetime of the vehicle.

## **1.3 SOC ESTIMATION**

There is not direct method to measure the SoC but instead there are methods to estimate the SoC [25],[26],[33].The main problem in designing an accurate SoC estimation system is the unpredictability of both battery behavior and user behavior [4]. For this reason one of the solutions is to use an adaptive system which is based on direct measurement, book keeping or combination of both. Example of the adaptive system is shown in Fig.1-1 which is called the Kalman filter method which is basically comparing the real battery we have with the battery model and by changing the parameter of the model until we get

the same physical output from both, then we can assume that all the parameters of the model equal the internal parameters of the real battery so the SoC of the real battery should be equal to the SoC of the battery model, beside this method there is also fuzzy logic and neural network methods.

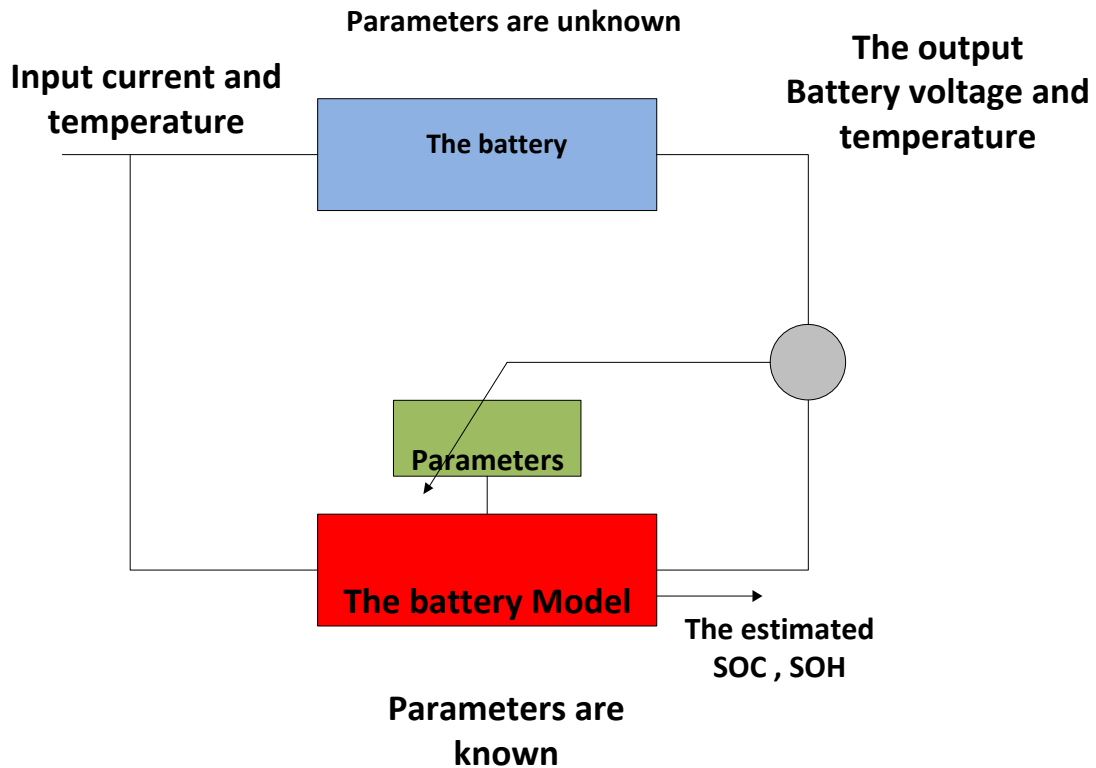


**Fig. 1-1** Kalman filter method for SoC estimation

## 1.4 BATTERY MODELING

Battery modeling is important in SoC estimation and also in simulation of the equalization circuits of the battery cells.

There are lot of methods to model a battery, some are based solely on electrochemistry such as Peukert equation, Shepherd model equation, Unnewehr universal model, and

other methods try to be more accurate on the internal capacitance in the battery such as dynamic lumped parameter battery model [8].

Introducing two battery models suitable for battery cell equalization simulation for the electrical vehicle system

### 1.4.1 RUN-TIME BATTERY MODEL

This model was chosen because of its simplicity and having a high precision in the range of SOC typically used in EV (from 40% to 80 %).

The proposed battery model shown in Fig.1-2 captures all the dynamic electrical characteristics of batteries: usable capacity (Ccapacity), open-circuit voltage (VOC), and transient response (RC network) all the relationship found in [20].

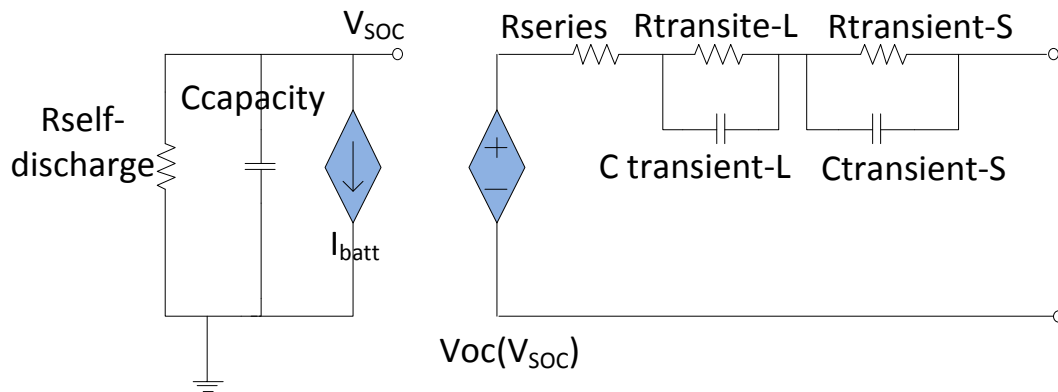


**Fig. 1-2** Run-time battery model

## 1.4.2 GENERIC BATTERY MODEL

The battery model is shown in Fig.1-3 assuming constant internal resistance and the model parameter can be easily extracted from the manufacturer discharge curve which allows for easy use for the model.

This model is included in SimPowerSystems library of the Simulink details of this model found in [21].

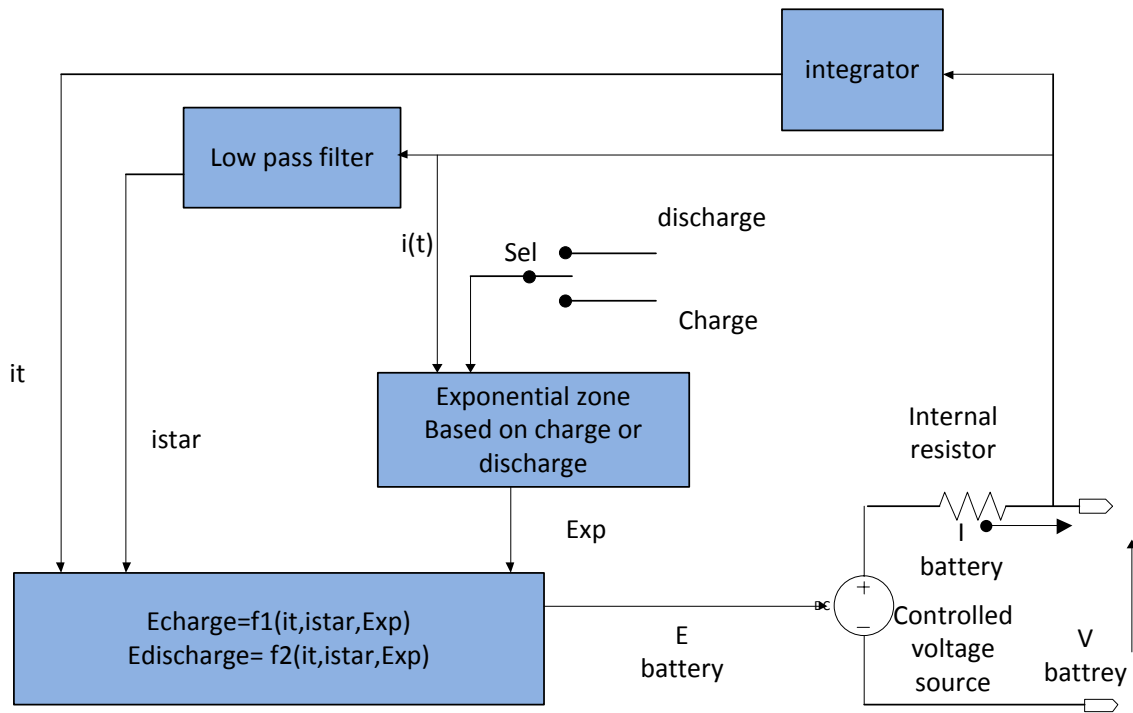


**Fig. 1-3** Generic battery Model



## **1.5 CONTRIBUTION OF THE THESIS**

The major contribution of this thesis includes:

- a) Proposing the use of the Serial Resonant Switched Capacitor Converter SRSCC as an active method to solve the battery cell equalization problem. For its advantage over the Switched capacitor in ZCS (low Switching losses) and its advantages over inductive based converter in low cost and weight
- b) proposing a technique for tuning the circuit using the microcontroller to achieve the zero current switching and as result reducing the MOSFET switching losses and achieving max equalization current
- c) proposing the controlled switching technique which allow the use of the current sharing method to reduce the equalization time significantly
- d) building a prototype of the proposed topology

## **1.6 THESIS OUTLINE**

The content of this thesis are organized into 5 chapters.

Chapter 1 include a brief introduction for the lithium-ion battery system and the parameter that should be monitored to ensure safe operation as well an introduction to the SoC estimation and Battery modeling.

Chapter 2 review the lithium-ion equalization problem and a brief review of the switching converter topologies used to solve this problem

Chapter 3 the proposed SRSCC topology including modes of operation, modeling and simulation

Chapter 4 the experimental setup and test results of the proposed topology with the use the microcontroller for tuning and controlled switching

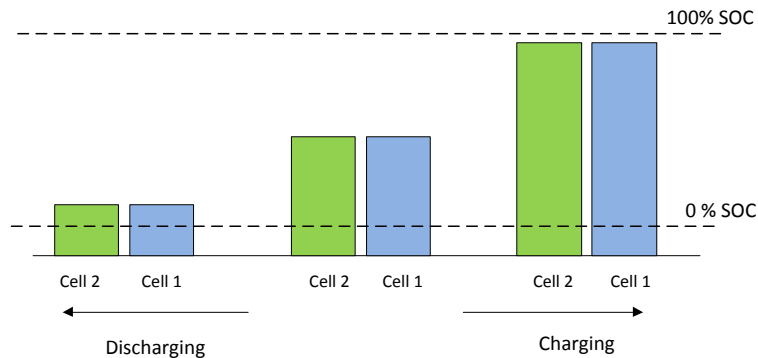
Chapter 5 summarizes the research conducted in the Thesis and presents the overall conclusion.

## CHAPTER 2

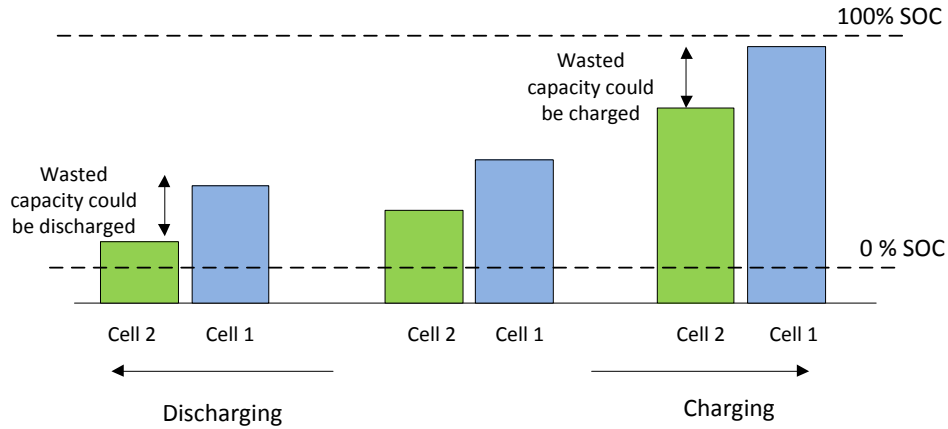
# REVIEW OF SWITCHED CONVERTER TOPOLOGIES FOR ELECTRIC VEHICLE BATTERY CELL EQUALIZATION

### 2.1 INTRODUCTION

Connecting the lithium-ion battery cells in series rise problems due to the imbalance voltage of the cells and this is caused by the difference of internal resistance of the cells, imbalanced state-of-charge (SOC) between the cells, degradation and the gradients of ambient temperature of the battery pack during charging and discharging, this imbalance in cells voltages can lead to severe decrease in storage capacity and in the worst case may be an explosion or fire [2].thus charge equalization for a series connected battery string is necessary to prevent these phenomena and extend the lifetime of the battery.



**Fig 2-1** Balance battery cells



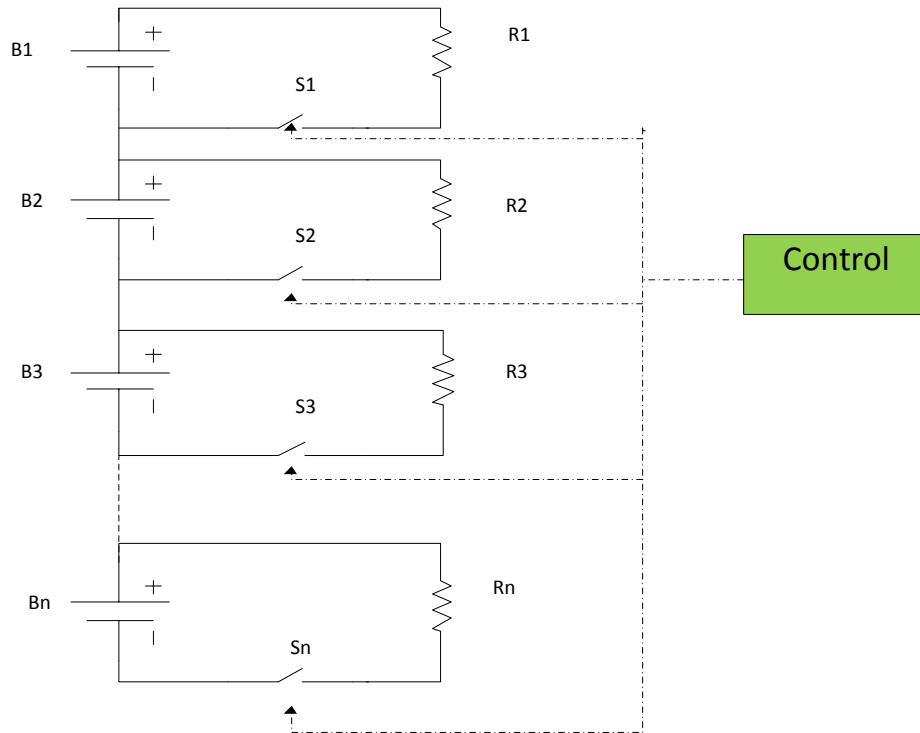
**Fig. 2-2** Imbalance battery cells

Fig. 2-1 is showing how the balanced cells are charging and discharging to their full capacity unlike imbalanced cells. As shown in Fig. 2-2, there will be always a wasted capacity that could be charged or discharged.

In the lead-acid batteries, the cell-to-cell imbalance can be solved by controlled overcharging [3]. It can be brought into overcharge conditions without permanent cell damage. The lithium-ion batteries cannot be overcharged. Hence, alternative methods are required.

These alternative methods for cell equalization include dissipative techniques and active cell balancing methods. The dissipative methods are based on getting rid of the extra charge in some cells by shunting the cells to dissipative resistors, as shown in Fig.2-3. This is not practical for hybrid electric and electric vehicles, due to the generation of heat and the loss of the power although its very appealing method for the HEV applications for its simplicity and low cost [36], [38]. There are also some active methods that are not

practical for Hybrid and Electrical Vehicles such as multicore transformers described in [3], [16],[24] due to the high cost and special built components.



**Fig. 2-3** Dissipative method commercially used in Vehicles

The alternative method to the dissipative method is using the Individual Cell Equalization ICE as shown in Fig.2-4, normally these ICE are DC-DC converters and this is showing The roll and the importance of the power electronics in achieving the cell balancing of the batteries, as in [24],[42]these DC-DC converter can be buck-boost, fly-back,  $C\hat{U}K$  or other topologies to transfer the extra charge from one cell to other with high efficiency .these topologies that are suitable for battery vehicle system will be reviewed next.

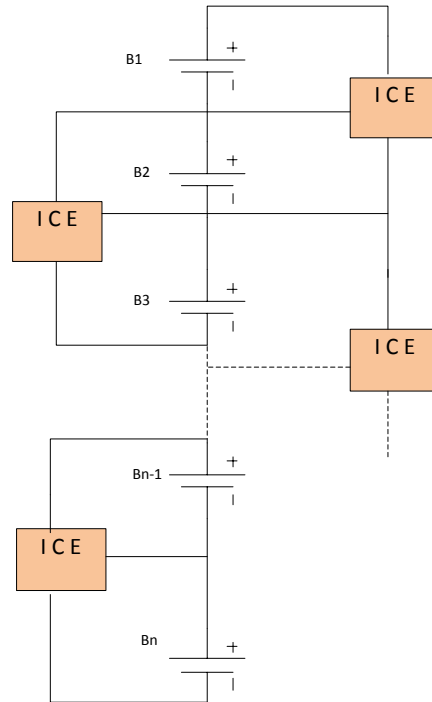


**Fig2-4** Individual cell equalization method

## 2.2 Modified CUK converter

In [10], [1] both uses CUK converter but the method in [1] uses the fuzzy logic control algorithm, it doesn't need for a mathematical model of the battery, the cell voltage balancing is performed by using a bidirectional DC-DC converter with energy transferring capacitance modified from the CUK converter as shown in Fig.2-5, the cell voltage are controlled by the driving pulse-width modulation signals corresponding to the respective cell voltage. The cell voltage difference in the battery strings and the controlled power MOSFET switches determine the direction of the energy transfer

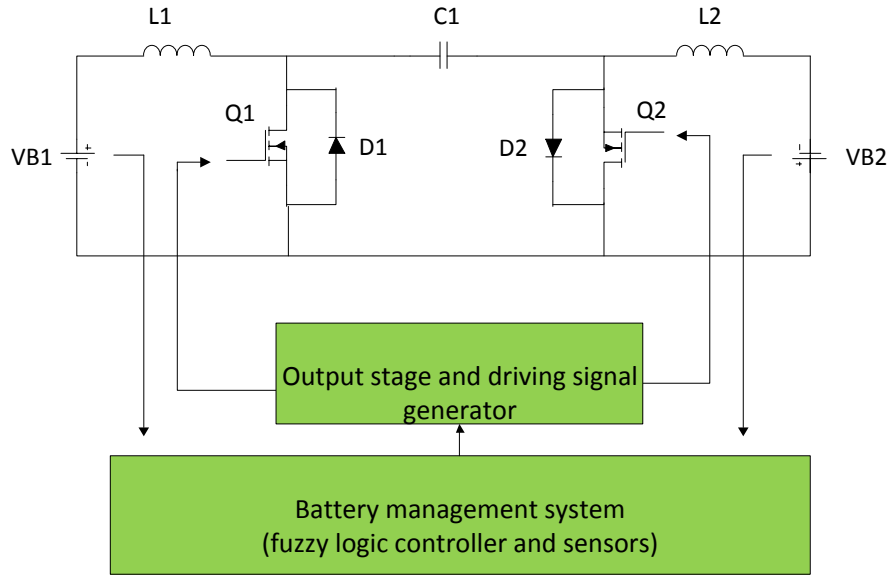


**Fig. 2-5** The proposed battery equalizer using modified CUK converter.

The initial voltage of the capacitor =  $VB1+VB2$

Assuming  $VB1 > VB2$  the sequence of operation will be as follow:

**1. For the period  $t_0 \leq t \leq t_1$**

Q1 is turned ON and the capacitor energy is transferred to VB2 and the inductor L1 stores the energy from VB1 as shown in Fig.2-6.

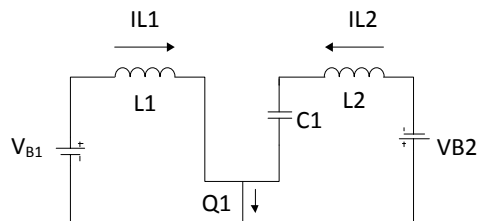


**Fig.2-6** Q1 is turned ON

$$VB1 = L1 \frac{di_{L1}}{dt}, \quad \text{where } i_{L1}(t_0) = I_0 \quad (2-1)$$

$$VB2 = -L2 \frac{di_{L2}}{dt} + \frac{1}{C1} \int i_{L2} dt, \quad \text{where } i_{L2}(t_0) = I_0 \quad (2-2)$$

$$VC1(t_0) = VB1 + VB2 \quad (2-3)$$

**2. For the period  $t_1 \leq t \leq t_2$**

Q1 is turned off and D2 is forced to turn on the capacitor energy is supplied by cell VB1 and the stored energy in L2 is still charged to cell VB2 as shown in Fig.2-7.

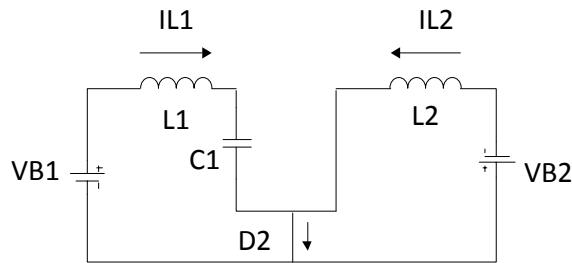


**Fig. 2-7** Q1 is turned OFF

$$VB2 = L2 \frac{di_{L2}}{dt}, \quad \text{where } i_{L2}(t_1) = I_P \quad (2-4)$$

$$VB1 = -L1 \frac{di_{L1}}{dt} + \frac{1}{C1} \int i_{L1} dt, \quad \text{where } i_{L1}(t_1) = I_P \quad (2-5)$$

$$VC1(t_1) = VB1 + VB2 \quad (2-6)$$



In the steady state the average of the charger balance of the capacitor over switching cycle is

$$i_{L1}(1 - D)T_s - i_{L2}DT_s = 0 \quad (2-7)$$

D is duty cycle and  $T_s$  is the switching period, which give the average currents for inductors as

$$I_{L1} = \left[ \frac{1}{2} \left( \frac{VB1}{L1} D^2 + \frac{Vc1-VB1}{L1} (1 - D)^2 \right) \right] T_s \quad (2-8)$$

$$I_{L2} = \left[ \frac{1}{2} \left( \frac{Vc1-VB2}{L2} D^2 + \frac{VB2}{L2} (1 - D)^2 \right) \right] T_s \quad (2-9)$$

The interesting thing in the proposed cell balancing control it can be designed in the CCM (Continues Current Mode) or in DCM (Discontinuous Current Mode) by the properly selecting of the switching duty as required.

### **2.3 Buck-boost and Quasi-resonant zero current battery equalizing**

Buck-boost method in cell equalization shown in Fig.2-8 has advantage over the dissipative method such as the high equalization efficiency, bidirectional energy transfer and a modular design but also it has some disadvantage such as the losses due to the hard-switching of the bidirectional dc-dc and the EMI emission in the battery charging system.

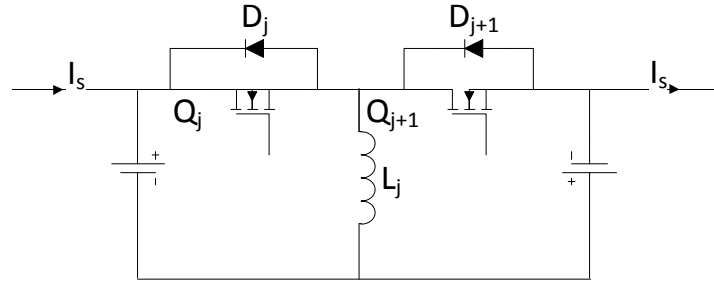


**Fig. 2-8** Buck-Boost Battery equalizer

In [9].[41] in order to reduce the losses of switching and lower the EMI Emissions it has been suggested to use zero-current soft switching technology based on the quasi-resonant converter So the result was the Buck-boost QRZCS battery equalizer circuit shown in Fig. 2-9.

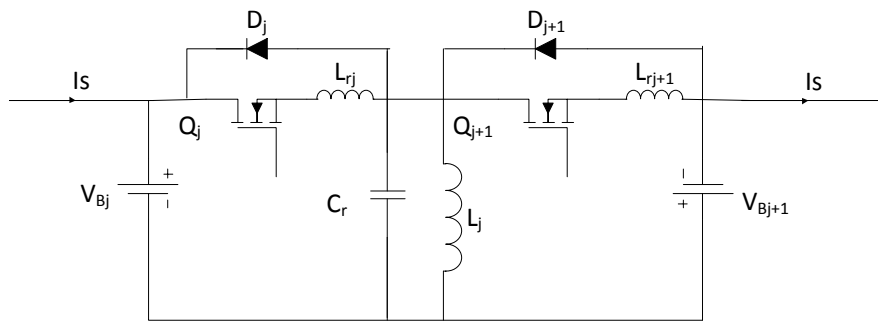


**Fig. 2-9** Buck-boost QRZCS battery equalizer circuit

But in order to minimize the number of passive inductance element and keep the same QRZCS topology he propose the Modified QRZCS Battery equalizer shown in Fig.2-10

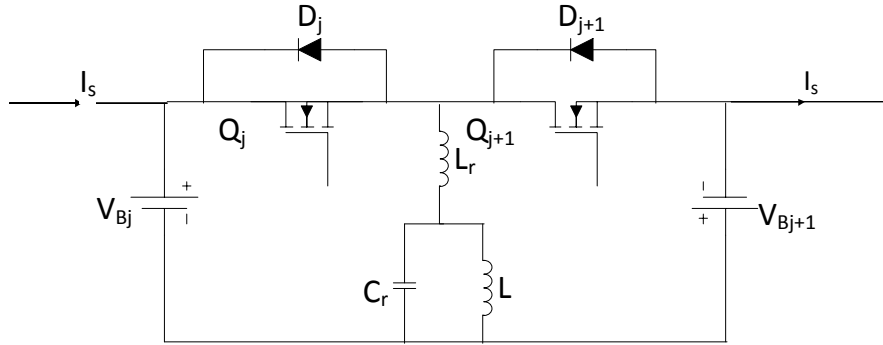


**Fig.2-10** The Modified QRZCS Battery equalizer

In order to analyze the Modified QRZCS circuit it is assumed that the main inductance  $L$  is sufficiently large to be considered as current supply, the semiconductor switches are ideal and the tank circuit reactive element are ideal.

Assuming  $V_{Bj} > V_{Bj+1}$ , then the equivalent circuit and switching waveform as Fig.2-11

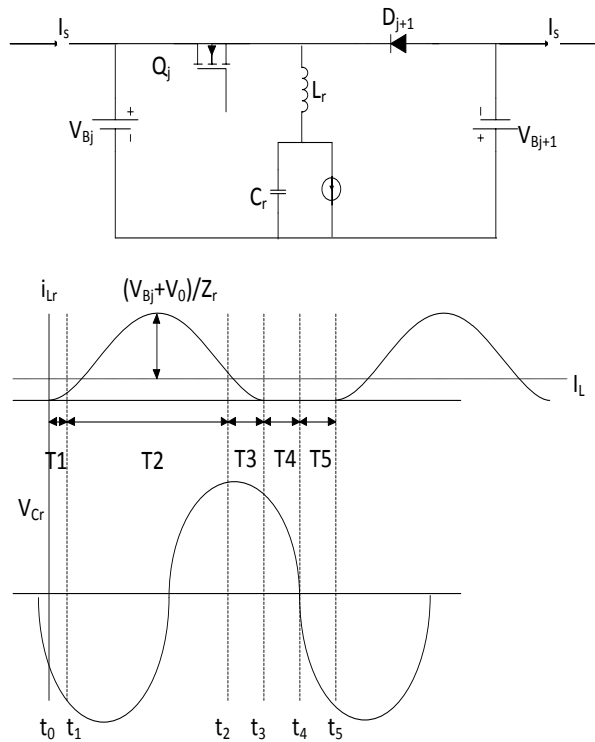


**Fig.2-11** The equivalent circuit and switching waveform

**1. For the Period  $t_0 < t < t_1$**

The main switch Qj will turn on and the current will flow to the resonant tank  $L_r$  and  $C_r$  to store energy in large inductor L as shown in Fig.2-12.

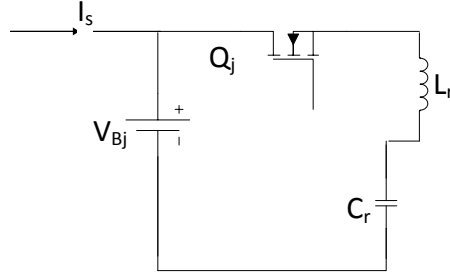


**Fig 2-12 QRZCS Period  $t_0 < t < t_1$**

Which gives  $i_{Lr} = \frac{V_{Bj}+V_0}{Z_r} \sin w_r t + (1 - \cos w_r t)I_L$  (2-10)

Where  $w_r = \frac{1}{\sqrt{L_r C_r}}$  is the resonant angular frequency and  $Z_r = \sqrt{\frac{L_r}{C_r}}$  is the normalize impedance. When  $t = t_1$ ,  $i_{Lr} = I_L$  then the time period

$T_1 = t_1 - t_0 = \frac{1}{w_r} \tan^{-1} \left( \frac{I_L Z_r}{V_{Bj}+V_0} \right)$  (2-11)

**2. For the Period  $t_1 < t < t_2$**

$Q_j$  is still turned on and the inductor current will increase to reach to peak value and substantially decrease until the main switch is turned off at  $t = t_2$  as in Fig.2-13.

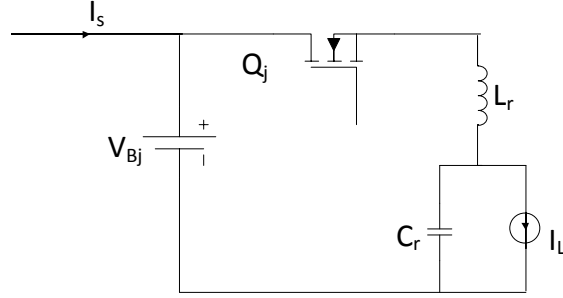


**Fig.2-13** QRZCS the Period  $t_1 < t < t_2$

$$T_2 = \frac{-1}{\omega_r} \sin^{-1}(I_L - I_0) \quad (2-12)$$

### 3. For the Period $t_2 < t < t_3$

When  $Q_j$  is turned off the resonant inductor current simultaneously switches to the body diode  $D_{j+1}$  which is forced to turn on and charges the cell  $V_{Bj+1}$  through the resonant tank  $L_r$  and  $C_r$  as shown in Fig.2-14.

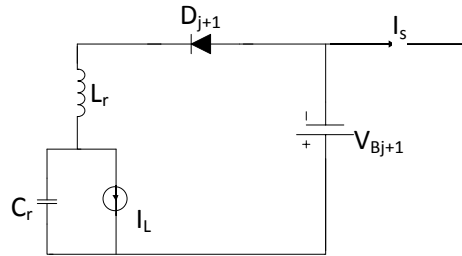


**Fig.2-14** QRZCS the Period  $t_2 < t < t_3$

$$i_{Lr}(t) = (I_0 - I_L) \cos(\omega_r(t - t_2)) - \frac{V_{Bj+1} + V_{cro}}{Z_r} \sin[(\omega_r(t - t_2))] + I_L \quad (2-13)$$

$$T_3 = t_3 - t_2 = \frac{1}{\omega_r} \left\{ \tan^{-1} \left[ \frac{Z_r \times (I_0 - I_L)}{V_{Bj+1} + V_{cro}} \right] + \sin^{-1} I_L \right\} \quad (2-14)$$

**4. For the Period  $t_3 < t < t_4$**

In this interval Q<sub>j</sub> and the diode D<sub>j+1</sub> are both turned off, the inductor current  $i_L(t)=0$ , the capacitor is discharged to the constant current source by  $I_L$  and the voltage across the capacitor will be  $V_{cr}(t) = V_{co} - \frac{1}{C_r} \int I_L dt$  the equivalent will be as Fig.2-15.

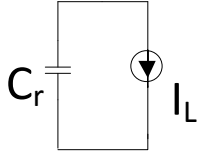


**Fig.2-15 QRZCS Period  $t_3 < t < t_4$**

$$T_4 = t_4 - t_3 = \frac{V_{co}C_r}{I_L} - \frac{1}{\omega_r} \left\{ \tan^{-1} \left[ \frac{Z_r \times (I_0 - I_L)}{V_{Bj+1} + V_{cro}} \right] + \tan^{-1} \left( \frac{I_L Z_r}{V_{Bj} + V_0} \right) + \sin^{-1} I_L - \sin^{-1}(I_L - I_0) \right\} \quad (2-15)$$

**5. For the Period  $t_4 < t < t_5$**

This is the free-wheeling the equivalent circuit identical as Fig.2-18 the sinusoidal voltage  $V_{cr}$  is substantially decreased to reach the negative peak it then increases until the next switching cycle the free-wheeling current is very small during the interval so the  $i_{Lr}(t)$  can be neglected

$$T_5 = t_5 - t_4 = \pi - \frac{1}{\omega_r} \left[ \tan^{-1} \left( \frac{I_L Z_r}{V_{Bj} + V_0} \right) - \sin^{-1} I_L \right] + \frac{V_{co}C_r}{I_L} \quad (2-16)$$

So the period of the entire cycle of the converter can be determined by

$$T_s = T_1 + T_2 + T_3 + T_4 + T_5 \quad (2-17)$$

And the switching frequency is  $f_s = 1/T_s$  and the conduction duty ratio  $D = \frac{T_1+T_2}{T_s}$

And the average inductor current  $I_L$  is

$$I_L = \frac{1}{\omega_e^2 T_s} \times \left\{ \left( \frac{V_{Bj}}{L_r+L} + \frac{V_0}{L} \right) \times (\cos \omega_e D T_s - 1) - \left( \frac{V_{Bj+1}}{L_r+L} + \frac{V_{cro}}{L} \right) \times (\cos \omega_e (1-D) T_s - 1) \right\} + \frac{T_s}{2(L_r+L)} \times [D^2 V_{Bj} - (1-D)^2 V_{Bj+1}] \quad (2-18)$$

## 2.4 fly-back equalizer and the modularized technique

In [12],[13] proposed a fly-back bidirectional cell equalizer for three cell battery with the ability to be modularized as shown Fig.2-16.

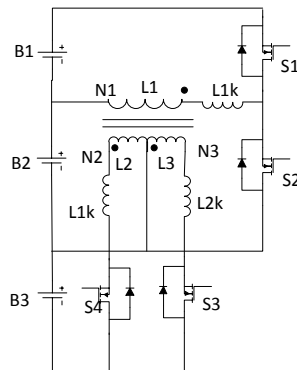


**Fig.2-16** Proposed fly-back equalizer

In [15] proposed another fly-back equalizer But in [2],[11] introduced the modularized concept in details ,which is basically divide the battery string in into M modules each module has N number of cells, the main advantage of this concept is lowering the voltage stress on the electronic devices and reduce the complexity of the controller .

In each module the cell equalizing is achieved by the fly-back converter that connected to each cell and the cell selection switch, this combination is called intra-module equalizer [11].

Due to the independent of intra-module balancing process the module balance is unstable to overcome this problem they used the Module Balancing Circuit which consist of transformers Model Balancing Transformers there secondary are connected in parallel and each primary is connected to a different intra-module equalizer, the proposed circuit can be shown in Fig.2-17.

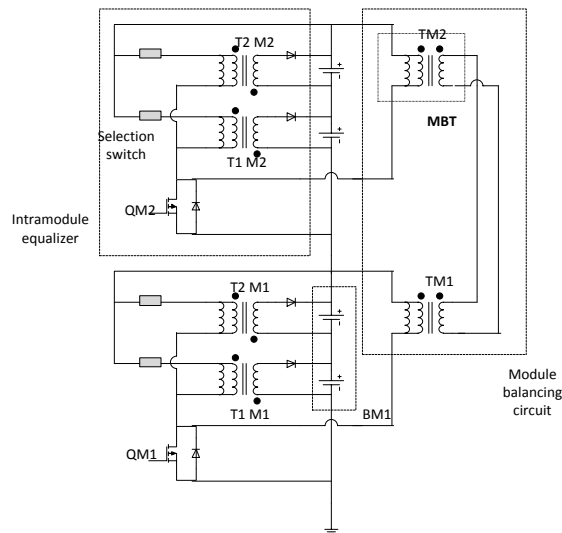


**Fig.2-17** Proposed modularized charge equalizer circuit consist with M=2 and N=2equalizer



In the proposed circuit its assumed that the MOSFET Switches are ideal except for their body diode and output capacitor and there is no losses in the selection switches and the leakage inductors  $L_{Kg2,M2}$  ,  $L_{Kg,M1}$  and  $L_{kg,M2}$  represent a parasitic inductive components of the transformers T2,M2 ,TM1 and TM2 respectively.

Assuming the BM2 is more undercharged than BM1 the operation sequence will be:

**1. For the Period  $t_0 < t < t_1$**

When both the MOSFET is turned ON ( $Q_{M1}$  and  $Q_{M2}$ ) the equivalent circuit will be as in Fig.2-18.

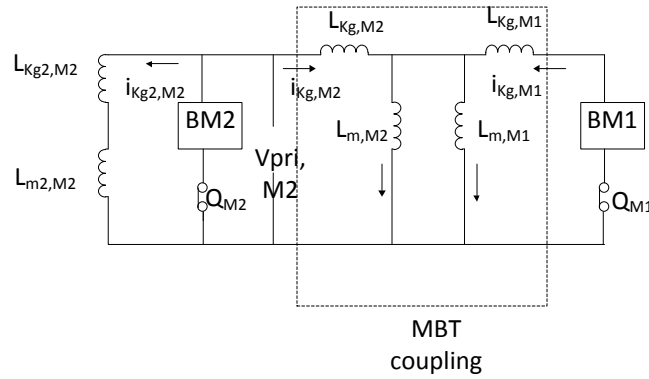


**Fig.2-18** Fly-Back equivalent circuit of period  $t_0 < t < t_1$

$$i_{Lm,M1}(t) = i_{Lm,M2}(t) + i_{Lm,M1}(t) - i_{Kg,M2}(t) \approx \frac{2V_{M1}}{L_{m,M1}}t + \frac{V_{M1}-V_{M2}}{2L_{Kg,M1}}t \quad (2-19)$$

**2. For the period  $t_1 \leq t \leq t_2$**

At this time both  $Q_{M1}$  and  $Q_{M2}$  will turn off synchronously.

$$v_{Coss,QM1}(t) \approx \frac{i_{Kg,M1}(t_1)}{C_{oss,QM1}}(t - t_1) \quad (2-20)$$

$$v_{Coss,QM2}(t) \approx \frac{i_{Kg2,M2}(t_1)}{C_{oss,QM2}}(t - t_1) - \frac{i_{Kg,M2}(t_1)}{C_{oss,QM2}}(t - t_1) \quad (2-21)$$

### 3. For the Period $t_2 < t < t_3$

At this period the rectifier diode D2M2 at the Secondary side of T2,M2 is turned ON.

$$i_{Lm,M1}(t) \approx i_{Lm,M1}(t_1) - \left(\frac{N_1}{N_2}\right) \frac{V_{B2,M2}}{L_{m,M1}} t \quad (2-22)$$

### 4. For the Period $t_3 < t < t_4$

This period starts when  $i_{Lm2,M2}$ ,  $i_{Lm,M2}$  and  $i_{Lm,M1}$  reach zero and resonance occurs until first period start over

## 2.5 The Switched Capacitor Battery Equalizing Topology

In [3],[14],[19],[22],[27],[31],[35] they all introduced the switched capacitor topology for battery cell equalizing in details, there was a misconception that Switched capacitor converters cannot handle high current and are inefficient but this proved to be wrong [14].

The switched capacitor converter is a good solution because of the eliminating the use of the inductive component which are usually large and cause high EMI and relatively heavy, and all this are important factors the HEV application.

Other advantages of using the switched capacitor converter is the simplicity because it doesn't need measurement circuits or closed loop feedback, and also the SCC is very efficient more than 90%, and it can be used during charging ,discharging or floating load

The only disadvantage of SCC is long equalizing time which considered very long compared to other inductive based converters.

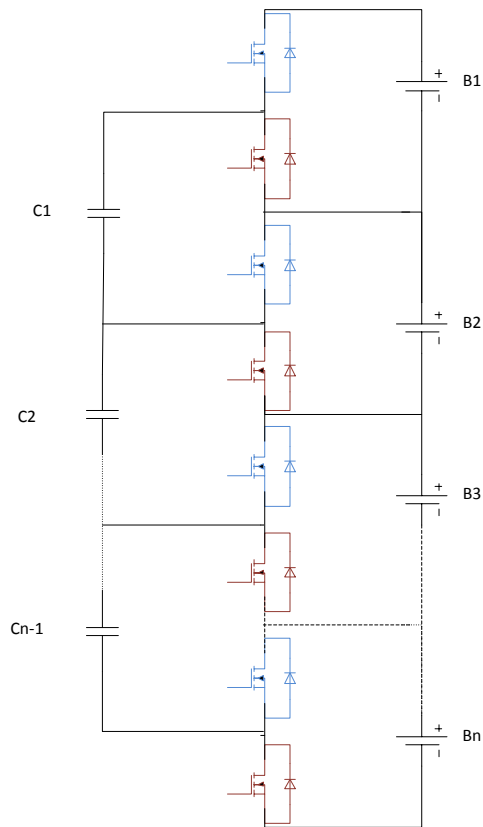


**Fig.2-19** SCC for battery cell voltage equalization

The equalization start by applying two complimentary signal of the PWM with duty cycle of 50% (actually the duty cycle is set to 45% to avoid shoot-through, case where the adjacent MOSFETs is on and shortened the cell) the signal is shown in Fig.2-20. Each signal to group of MOSFETs and the charge will shuttle from one cell to another based on the voltage difference between them.

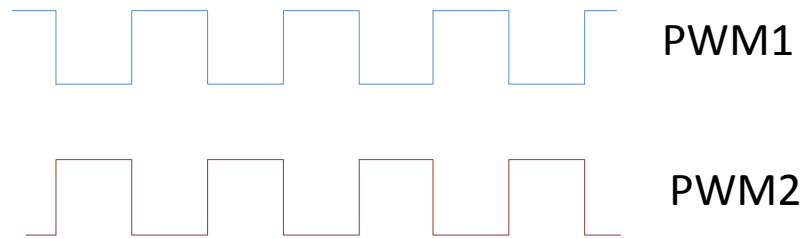


**Fig.2-20** Two complimentary PWM signal with Duty cycle = 50%

## 2.6 Summary

This chapter was a review of the most popular switching converter topologies to solve the lithium-ion battery cell equalization problem of the imbalance between the cells in the Hybrid and Electrical Vehicles battery system. So instead of using the dissipative method of shunting a dissipative resistor across the cell during charging, we reviewed the use of CUK converter and modified Buck-Boost converter to work as QRZCS and also the use of fly-back converter which are all inductive base type, in the other hand we reviewed switched capacitor converter which inductorless based converter which means less cost and less weight, and the SRSCC proposed by this thesis actually is a modification of the Switch Capacitor converter.

# **CHAPTER 3**

## **The Proposed Serial Resonant Switching Capacitor Converter**

### **SRSCC**

#### **3.1 INTRODUCTION**

The Serial Resonance Switched Capacitor Converter SRSCC in [32],[39],[40] and shown in Fig.3-1 is very similar with the conventional switched capacitor converter shown in Fig.2-19, the only difference between the two circuits is a small inductance. But this added inductance change the behaviour of the circuit and give it some advantages, one of these advantages is lowering the EMI [34],[37]. The inductance will prevent the capacitor current from changing fast, instead the capacitor current will change gradually to maximum value and then to zero and then to maximum value in the negative (when the energy is transferred from the capacitor to the inductance). If the MOSFET is switched at the point where the current is zero then the ZCS is achieved (also known as soft switching) and this will help to reduce the power switching loss which is very important issue especially at high switching frequencies.

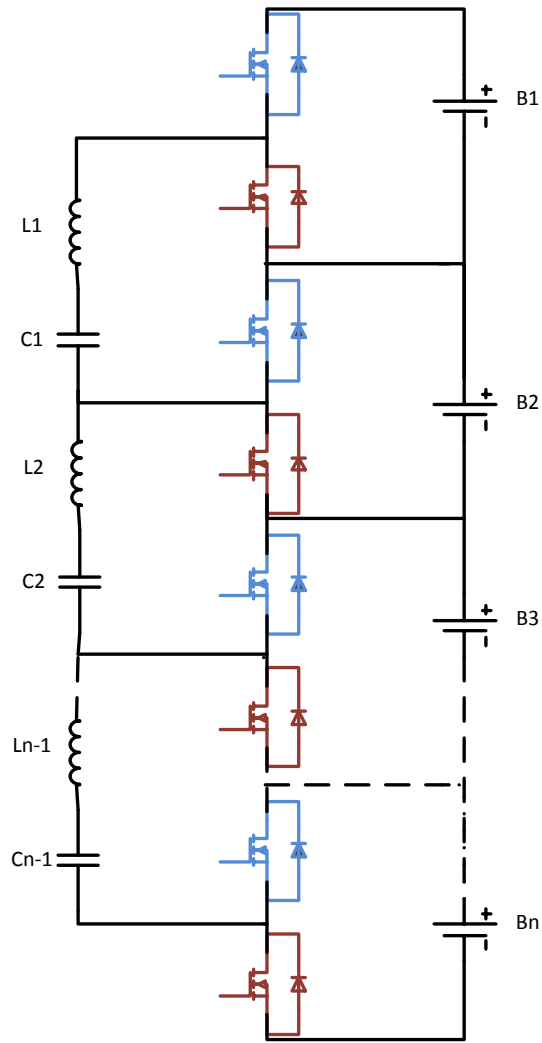


**Fig3-1** Resonance Switched Capacitor battery cell equalization Circuit

Soft switching is switching the MOSFETs transistors OFF at zero current (or zero voltage not this case) to get zero power loss and reducing the switching ON losses during the switch ON of the transistor, Fig.3-2 and Fig.3-3 is illustration to show the difference

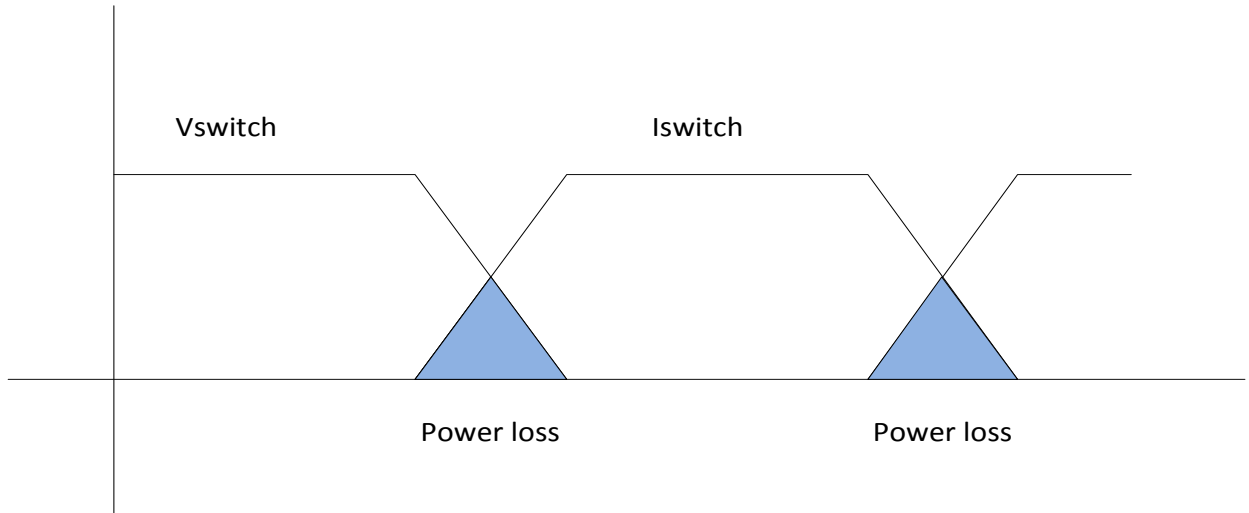


**Fig.3-2** Power loss in hard-switching of the MOSFETs

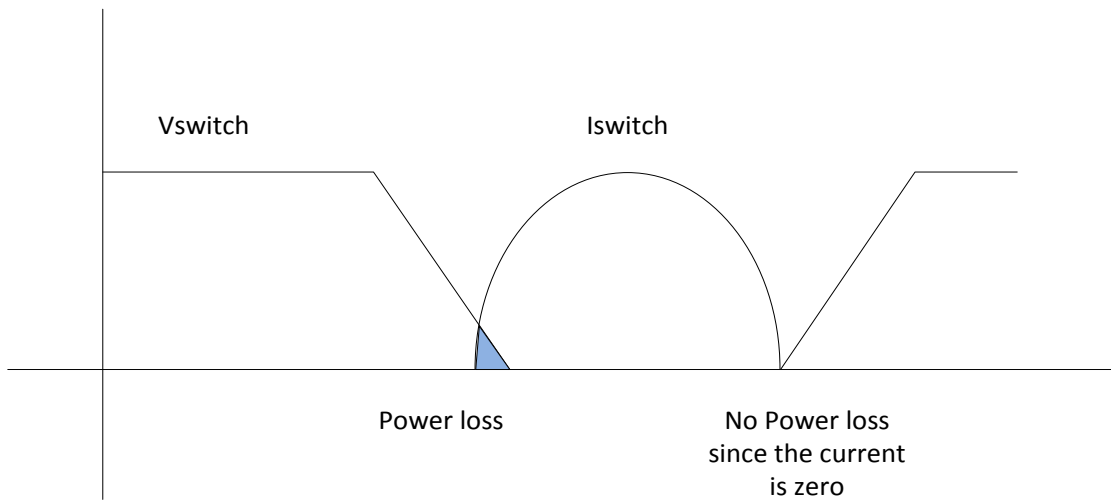


**Fig.3-3** The power loss of the MOSFETs in ZCS

Fig.3-4 is showing simulation results of the current and the voltage of the MOSFET when the Gate signal is applied

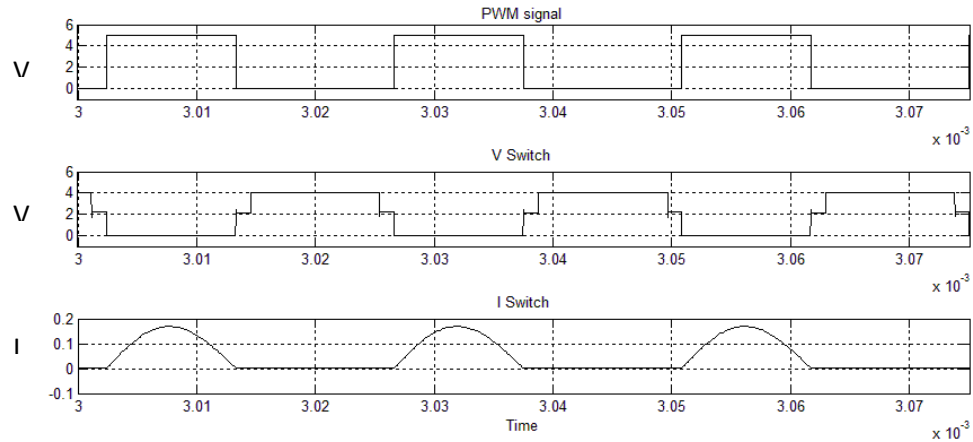


**Fig.3-4** MOSFET waveforms

### 3.2 Modes of Operation

The Serial Resonance Switched Capacitor Converter SRSCC in the equalization circuit has two states, state A and state B.

**State A** is shown in Fig.3-5, assuming  $V_{B1} > V_{B2}$  the battery with higher voltage will charge the energy transfer elements (capacitor and inductance).

Even when  $V_{B2} > V_{B1}$  the sequence of gating of the MOSFETs will be same but the current will be in the opposite direction of the Fig.3-4 because it depend on the voltage differences between the cells.



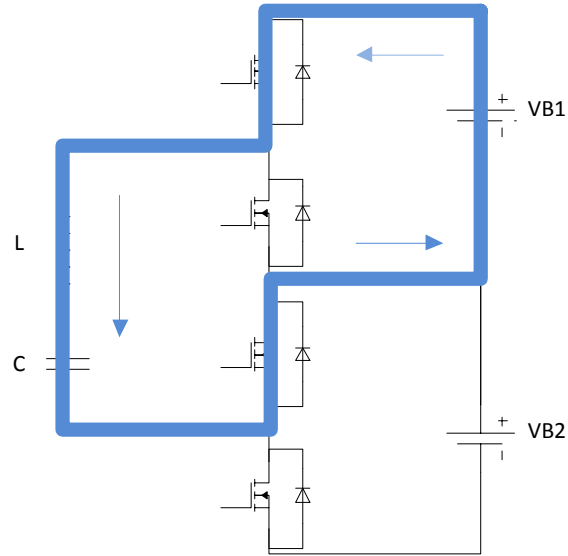


**Fig.3-5** State A charging the transfer elements

**State B** shown in Fig.3-6, the energy transfer element discharges the current to the cell with lower voltage.

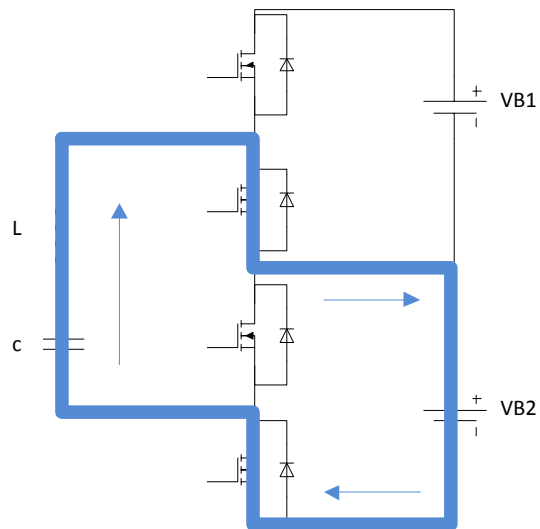


**Fig.3-6** State B discharging the energy transfer elements to the battery cell

### 3.3 Mathematical Modeling

The circuit analysis is done based on 2 cell and assuming  $V_{B1} > V_{B2}$

So for State A shown in Fig.3-4 the capacitor C will start charging, and state equation of the resonance current  $i_{res}$  will be

$$i_{res} = C \frac{dV_c}{dt} \quad (3-1)$$

$$L \frac{di_{res}}{dt} + V_c = V_{B1} \quad (3-2)$$

And the solutions are

$$V_c = V_{B1} + V \cos(\omega t + \theta) \quad (3-3)$$

$$i_{res} = I \sin(\omega t + \theta) \quad (3-4)$$

Where V is the amplitude of the capacitor voltage and I is the amplitude of resonance current.

For state B shown in Fig. 3-5 the capacitor will start to discharge and the state equation will be

$$i_{res} = C \frac{dV_c}{dt} \quad (3-5)$$

$$L \frac{di_{res}}{dt} + V_c = V_{B2} \quad (3-6)$$

And the solutions are

$$V_c = V_{B2} - V \cos(\omega t + \theta) \quad (3-7)$$

$$i_{res} = -I \sin(\omega t + \theta) \quad (3-8)$$

For the resonance analysis assuming switches are ideal and capacitor has initial voltage  $V_{c \text{ int}}$  for State A the equation (3-2) will become

$$L \frac{di_{res}}{dt} + V_{c \text{ int}} = VB1 \quad (3-9)$$

And resonance current amplitude for state A  $I_A$  will be

$$I_A = \frac{VB1 - V_{c \text{ int}}}{\omega L} = (VB1 - V_{c \text{ int}}) \sqrt{\frac{C}{L}} \quad (3-10)$$

And maximum voltage across the capacitor  $V_{c \text{ max}}$  will be

$$V_{c \text{ max}} = 2VB1 - V_{c \text{ int}} \quad (3-11)$$

For State B the amplitude for resonance current  $I_B$  will be

$$I_B = \frac{V_{c \text{ intB}} - VB2}{\omega L} = (V_{c \text{ intB}} - VB2) \sqrt{\frac{C}{L}} \quad (3-12)$$

Where  $V_{c \text{ intB}}$  is the initial capacitor current on discharging

And the minimum voltage across the capacitor  $V_{c \text{ min}}$  will be

$$V_{c \text{ min}} = 2VB2 - V_{c \text{ int}} \quad (3-13)$$

Taking into the account the drop voltage across the switches  $V_d$  and considering the total resistance in the path of the current  $R_{\text{Total}}$

$$R_{\text{Total}} = 2R_{ds \text{ on}} + R_{ESR} + R_L + R_{pcb} \quad (3-14)$$

The resonant current for State A will be

$$i_{res A} = \frac{VB1-Vd-V_{c int}}{w_r L} e^{-\rho t} \sin w_r t \quad (3-15)$$

And for State B

$$i_{res B} = \frac{V_{c int B}-VB2-Vd}{w_r L} e^{-\rho t} \sin w_r t \quad (3-16)$$

Where  $\rho = \frac{R_{Total}}{2L}$  and  $w_r = \sqrt{\frac{1}{LC} - \rho^2}$

And maximum capacitor voltage will be

$$V_{c max} = V_{c int} + \frac{VB1-Vd-V_{c int}}{(\rho^2+w_r^2)LC} (1 + e^{-\rho\pi/w_r}) \quad (3-17)$$

And the minimum will be

$$V_{c min} = V_{c int B} - \frac{V_{c int B}-VB2-Vd}{(\rho^2+w_r^2)LC} (1 + e^{-\rho\pi/w_r}) \quad (3-18)$$

So the circuit is damp oscillation.

### 3.4 Circuit Design and Simulation

Starting the design of the SRSCC circuit by choosing a large value of Q (resonance Quality Factor) the higher the value of Q the closer the current shape to the Sinusoidal wave actually closer to quasi Sinusoidal wave since the duty cycle  $D < 50\%$  to avoid current shoot through , So Q is chosen to be  $Q = 20$ . And choosing the switching Frequency  $f_{sw} = 40$  kHz and assuming the  $R = 15m\Omega$ .

From equations (3-4) and (3-5) the value of inductance L and the capacitor C can be calculated.

$$Q = \frac{2\pi f_r L}{R} \quad (3-4)$$

$$f_r = \frac{D}{\pi\sqrt{LC}} \quad (3-5)$$

Where R is the total resistance in the path of the current (ESR of capacitor, RDS on MOSFETS, resistance of the tracks and the Resistance of the inductance) .  $f_r$  is the Resonance Frequency, and D is duty cycle = 45%. To achieve the soft switching we must have  $f_{sw} = f_r$ .

The inductance is calculated to be  $L = 1.2\mu H$  and capacitor to be  $C = 10\mu F$ .

SIMULINK of MATLAB was used to simulate the circuit of 4 battery Cells. The battery cells were modeled using the Generic Battery Model which is already in the Simulink library.

Fig. 3-6 is showing the simulation results of the current waveform when  $f_{sw} < f_r$

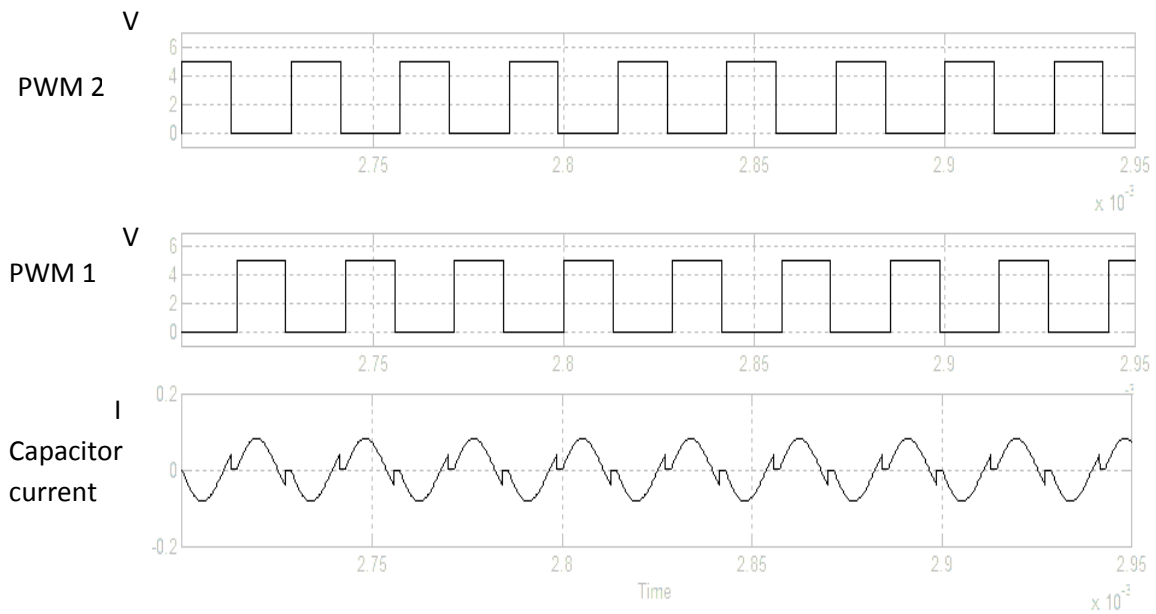


**Fig.3-7** The current waveform when  $f_{sw} < f_{res}$

It can be noticed from Fig.3-7 that the switching of the MOSFET is not at the point when the current is zero so there will be a switching losses and this show the importance of the tuning.

Fig.3.8 is showing the simulation results of the circuit when  $f_{sw} = f_r$  (tuned).it can be noticed that the zero current switching is achieved and current waveform is quasi sinusoidal wave since the Duty Cycle  $D = 45\%$  to avoid the current shoot through (in the experimental setup)

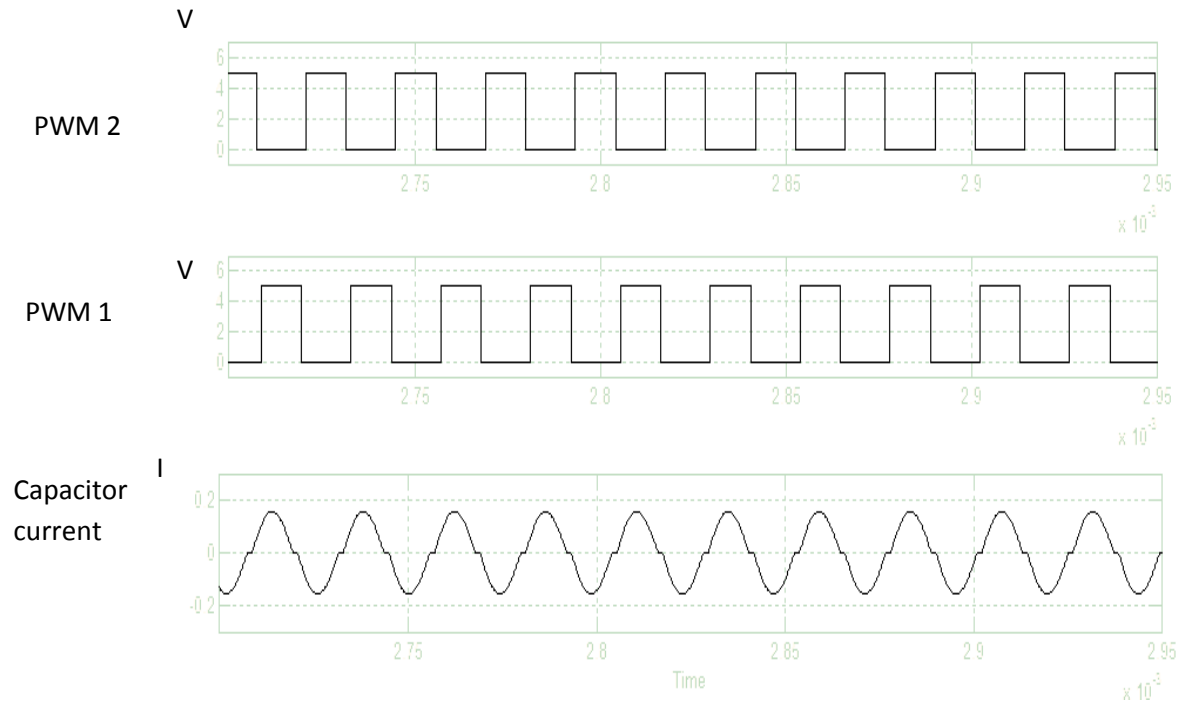


**Fig.3-8** Zero current switching when  $f_{sw} = f_r$

### 3.4.1 Controlled Switching and Current Sharing

In the Serial Resonance Switched Capacitor SRSCC and the conventional Switched Capacitor the switching of the MOSFET is done by applying two PWM signals one for the set of the MOSFETs of Charging and the other for the set of the MOSFETs of Discharging and based of the voltage difference between the adjacent cells the energy shuttle between the cells .

Every lithium-ion battery system must have BMS (Battery Management System) to supervise the charging and discharging of the battery and monitor the Temperature and the voltage of each cell, and this is done by a microcontroller. we can use the same

microcontroller to achieve controlled switching allowing to switch only the MOSFETS of the cells that need to be equalized saving on the power loss of the MOSFETS of the cell doesn't need equalization , and also allowing the use the current sharing method to reduce equalization time which is relatively high in switched Capacitor equalization topologies.

By using divide and conquer principle the equalization control can be divided as shown in Fig 3-9 chaining equalization control

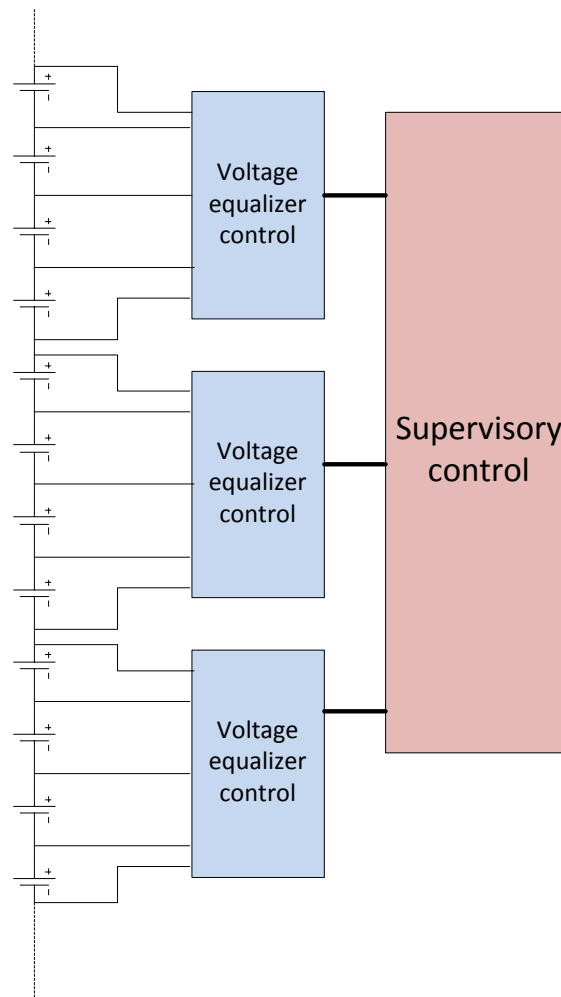


**Fig 3-9** Chaining equalization control



The number of cells to be controlled by each microcontroller depends on the designer. In our case, the number of cells chosen was 4, so the circuit will be as shown in

Fig 3-10

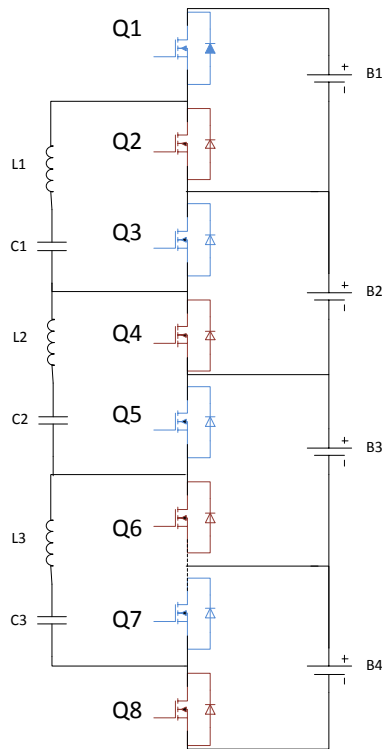


**Fig 3-10** Four cell SRSCC equalization

Here the microcontroller reads the voltages of the cells and based on their value the microcontroller enables only the MOSFETs for the equalization of the targeted cells.

Fig 3-11 is showing the proposed algorithm for equalization.

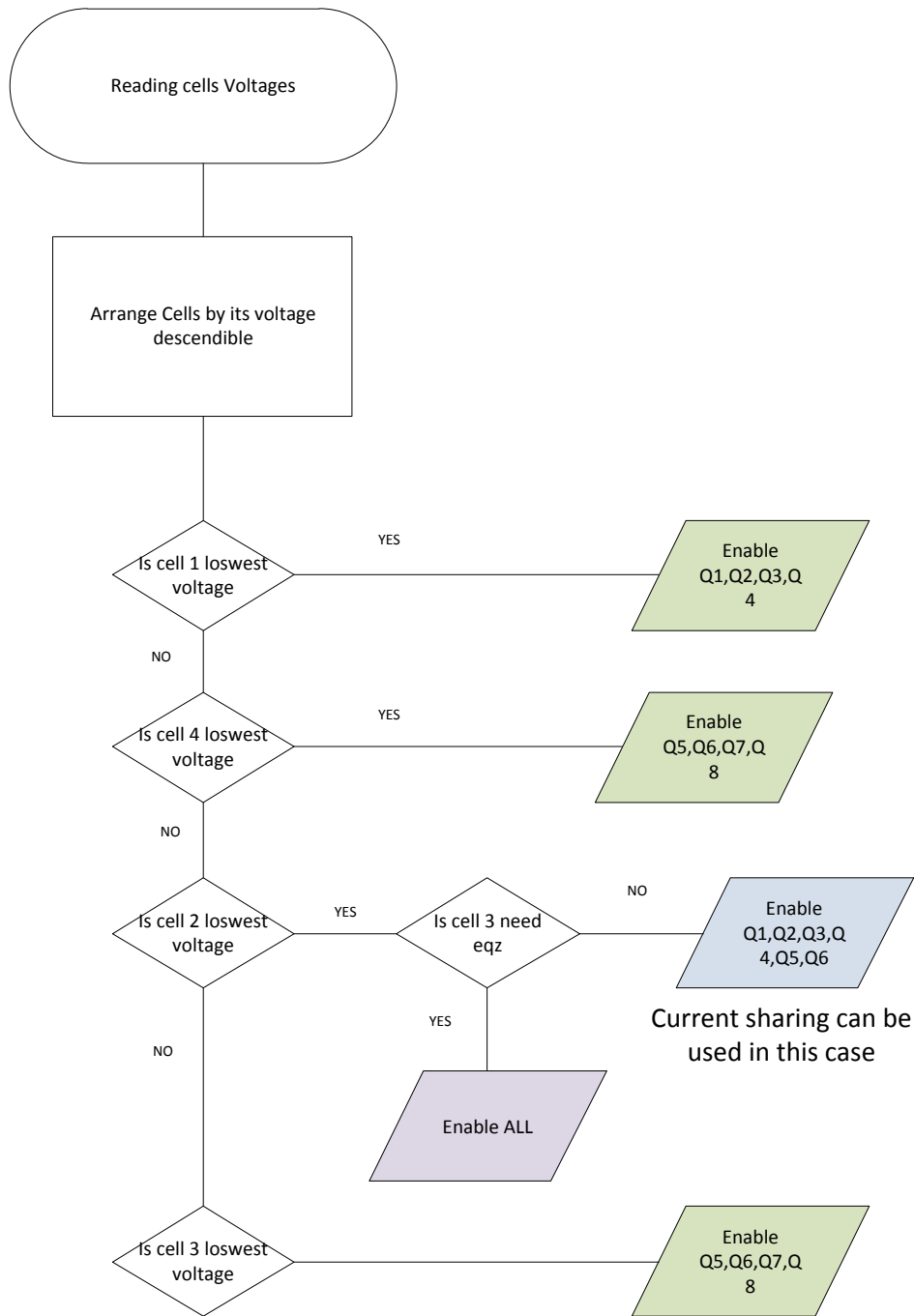


**Fig 3-11** The proposed algorithm for equalization

The proposed current sharing method allow the equalization between the two adjacent cells of both side not only one as in the conventional methods and this has the impact to reduce the equalization time significantly.

Assuming voltages of B1 and B3 > voltage of B2, the current sharing switching method also has two state.

State A shown in Fig.3-12 when B1 is charging the energy transfer elements L1 and C1 through Q1 and Q3 while at the same time the energy transfer elements L2 and C2 is discharging to B2 through also Q3 and Q5.

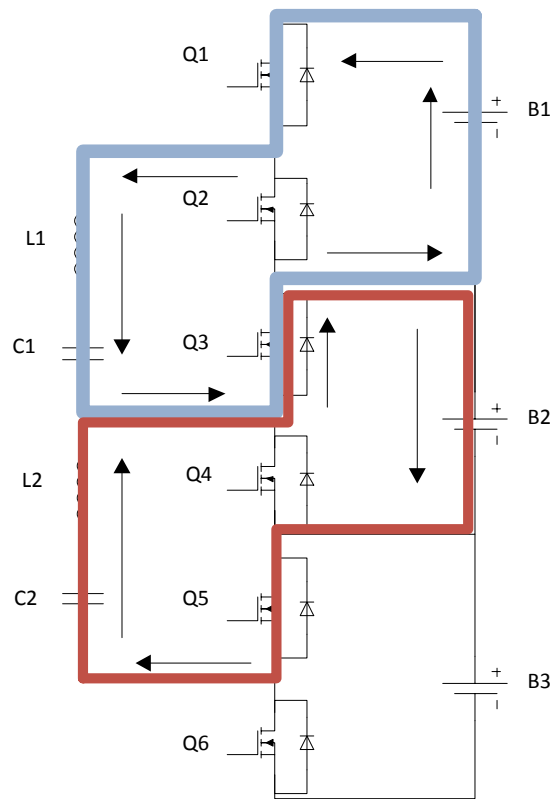


**Fig.3-12** State A of current sharing switching method

In state B shown in Fig.3-13 the transfer elements L1 and C1 is discharging the current to B2 through Q2 and Q4 while at the same time B3 is charging the energy transfer elements L2 and C2 through also Q4 and Q6.

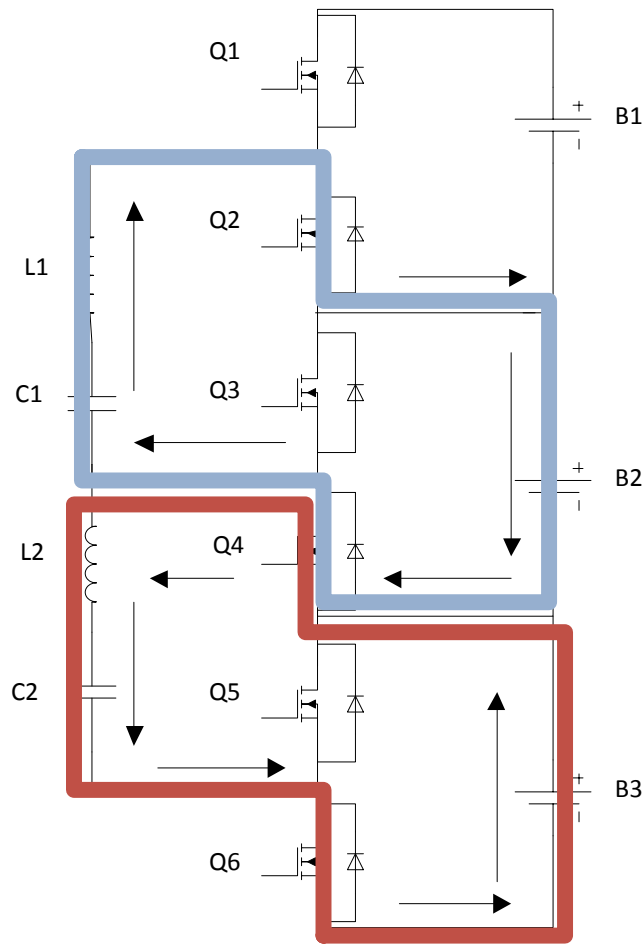


**Fig.3-13** State B of current sharing switching method

The selection of the MOSFETs should handle the extra current that going through when using the current sharing method.

The improvement in the equalization current between the conventional method and the current sharing can be shown in the simulation results of the current of the Battery cell

B2 as shown in Fig.3-14 and Fig.3-15. We can notice that the equalization current go to cell B2 not only in state A as in Fig.3-11 but both state A and State B as shown in Fig3-12. Please notice that these currents are entering B2, are the equalization currents.

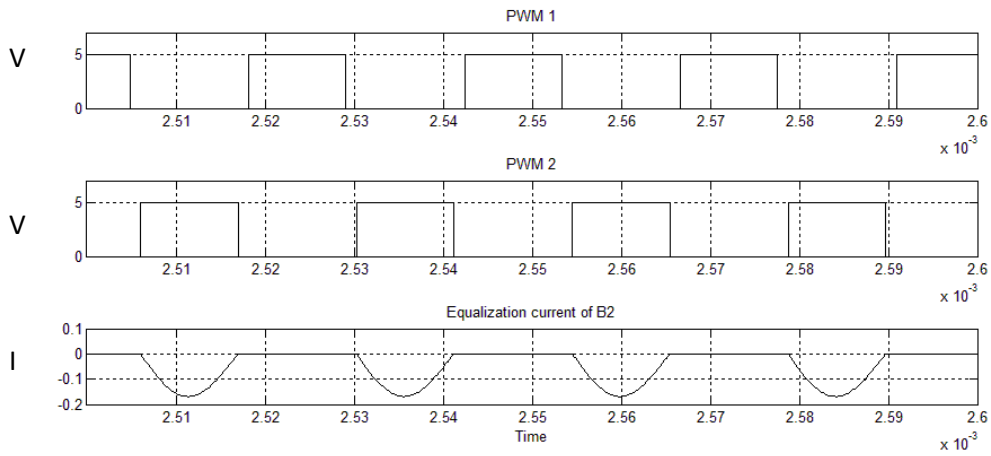


**Fig.3-14** B2 equalization current of the conventional method

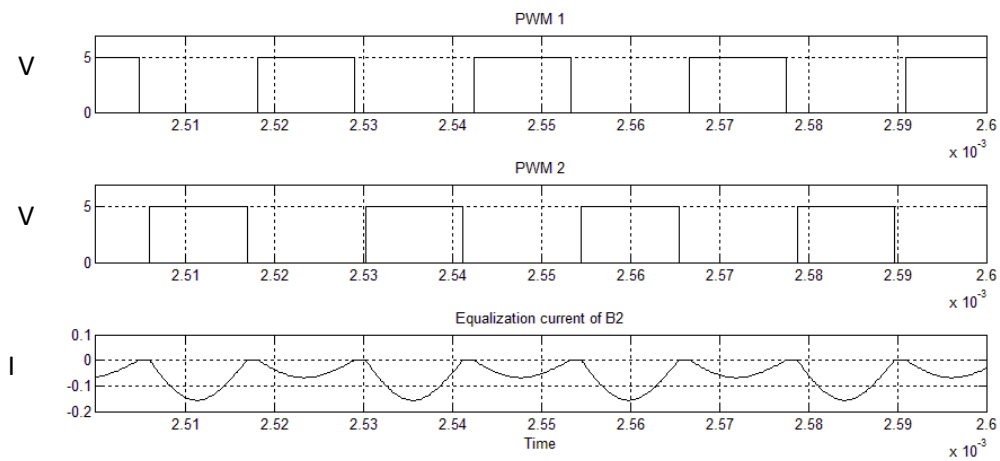


**Fig.3-15** B2 equalization current of the current sharing method

### 3.4.2 Equalization Time

Simulation the circuit until the cells equalize is not practical because it take very long time (weeks to simulate 5000 second) even by changing the battery model by using the Run-Time model for the lithium-ion cell instead of the generic battery model .so instead, the simulation is done to show the trajectory of the equalization current by modeling the battery cells with high value capacitor (10F) at no load .

Fig.3-16 shows the trajectory of the conventional method and Fig.3-17 show the trajectory of the current sharing method.

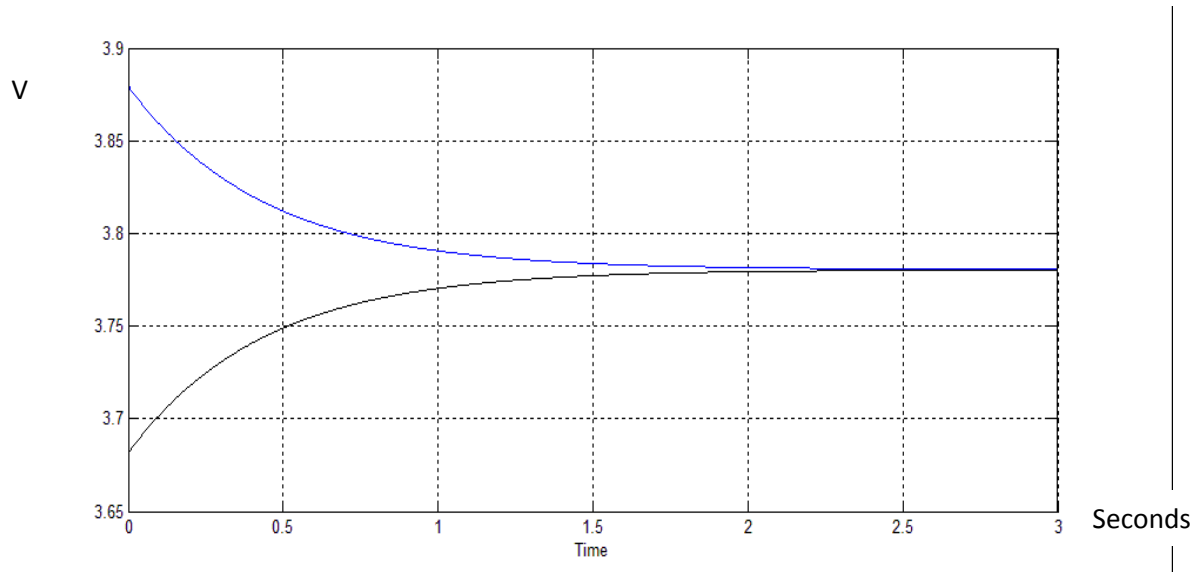


**Fig.3-16** Voltage equalization trajectory for conventional method(time in sec)

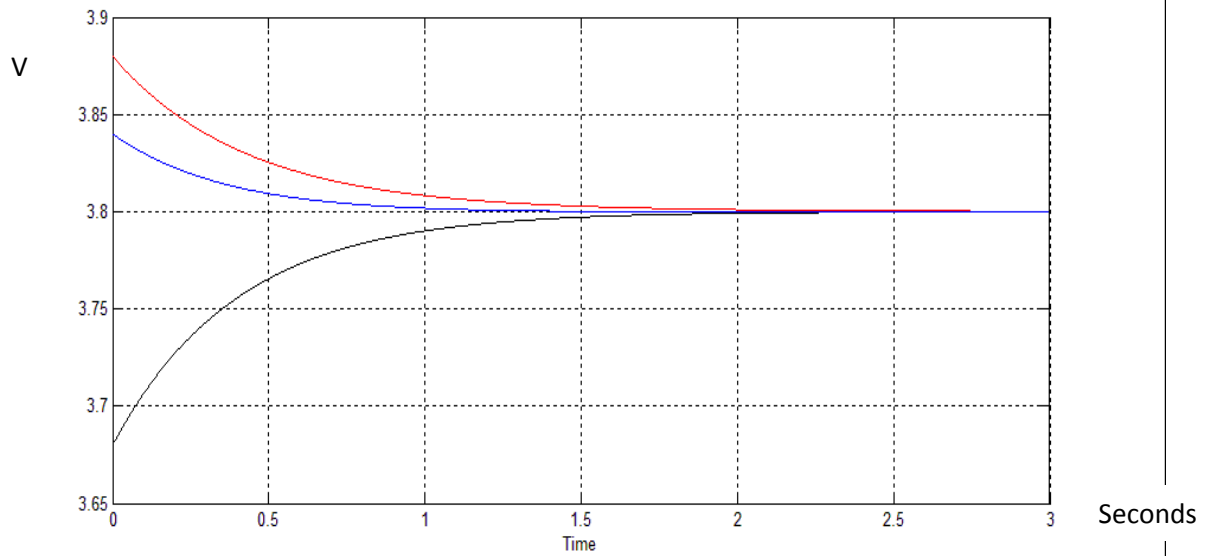


**Fig.3-17** Voltage equalization trajectory for current sharing method (time in sec)

It can be noticed from comparing Fig.3-16 and Fig.3-17 that equalization time in current sharing method is lower than the conventional method. In conventional method the equalization reached about 3.77 volt in 3 second but from Fig.3-14 it can be seen that B2 reached the 3.77 volts in less than 1 second or less than half the time of the conventional method .reducing the equalization time is very important since the its relatively high in the capacitor switching based converters.

### 3.5 Summary

In this chapter the proposed SRSCC has been introduced showing the two states of the circuit .a mathematical model of the circuit is introduced in the time domain using state space averaging theory.

It's also shown the importance of the tuning to achieve the zero current switching.

It was also showed the controlled switching method that allowed the use of the current sharing method to reduce the equalization time significantly.

Simulation also showed the trajectory of the voltages of the cells for both methods



# CHAPTER 4

## EXPERIMENTAL SETUP AND TEST RESULTS

### 4.1 INTRODUCTION

After proving in the simulation that the concept of SRSCC for equalization is working it's time to build the circuit in the lab.

This prototype has used four battery cells each of capacity of 2.2 A-h.

The circuit was built around the PIC18F46K80 microcontroller which has a 12bit resolution ADC, two comparators, and four CCP (Capture/Compare/PWM) modules.

The N-MOSFET was of BUK952R8-30B Type which was chosen of its very low resistance RDS-ON about 2.4m $\Omega$ .

Actually choosing the component was based on the component that has lower resistance values that are available because the value of R total (ESR of capacitor, RDS ON of the transistor, inductance resistance and the resistance of the tracks of the board) has great effect on the value of equalization current.

Fig.4-1 is showing the board built for four cells battery equalization

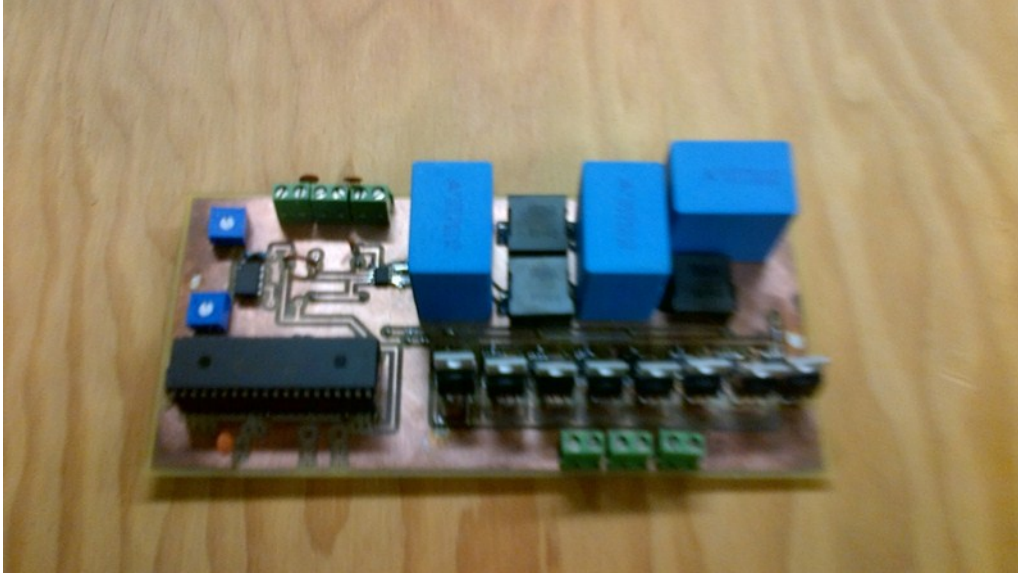


**Fig.4-1** The prototype board for the four cell battery equalization using SRSCC

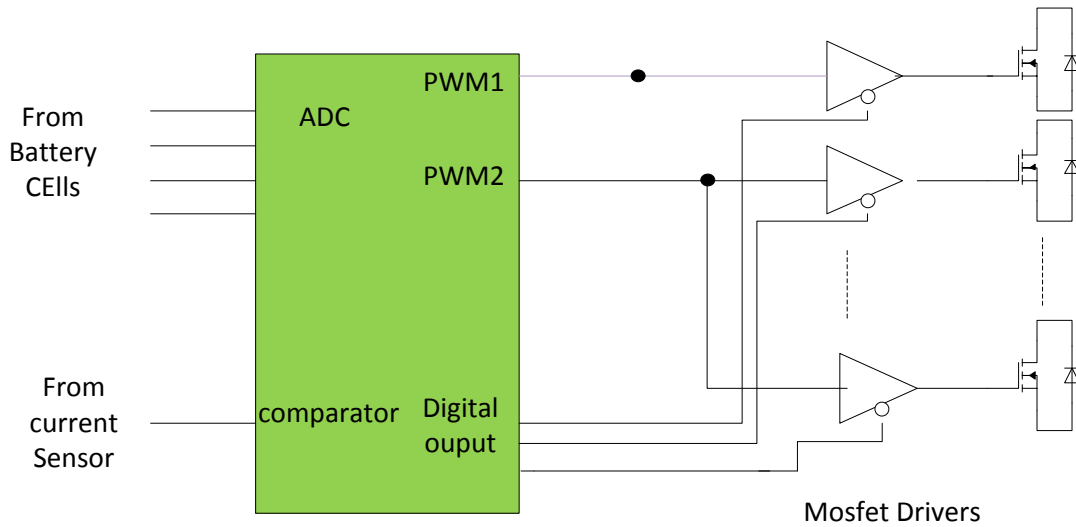
## 4.2 CONTROL CIRCUIT AND TUNING

Fig.4-2 is showing the control circuit diagram and the role of the microcontroller in the tuning and the switching of the MOSFETs.

The voltage signal from the current sensor of the capacitor (connected in serial with capacitor) is fed to the comparator module built in the microcontroller and compared with internal generated reference voltage the output of the comparator is pulse wave is fed to the CCP module of the microcontroller working in capture mode to calculate the width of the pulse as shown in Fig.4-3. From the calculated width of the pulse and using equation (4-1) the microcontroller calculate the exact Resonance Frequency and set the switching Frequency  $f_{sw}$  to value of  $f_r$ .

$$f_r = f_{mes} \times D \quad (4-1)$$

Where  $f_r$  is the resonance Frequency,  $f_{mes}$  is the measured frequency and D is the dutycycle.



**Fig.4-2** Control circuit diagram

There is one condition in order the microcontroller can calculate the exact resonance frequency is that the starting switching frequency must be lower than the designed resonance frequency. And since we are using single current sensor we are assuming the component will have the exact same value

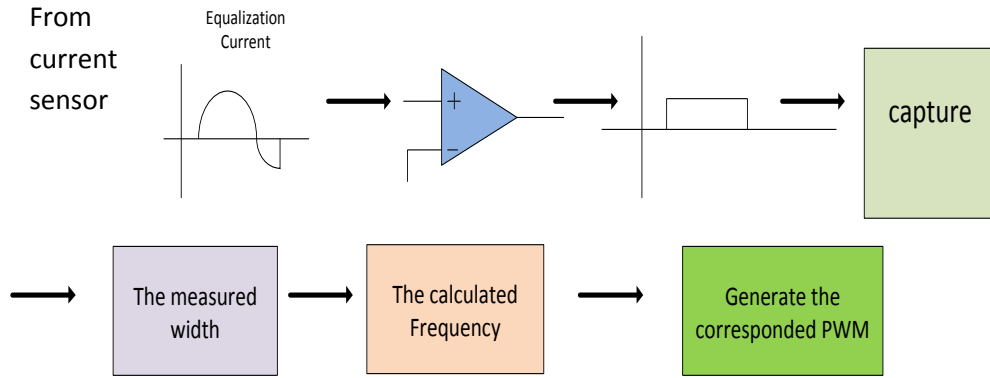


**Fig.4-3** Steps of tuning

The starting PWM frequency of the microcontroller was set to 35 kHz which is lower than the designed resonance Frequency  $f_{res} = 40$  kHz. Fig.4-4 and Fig.4-5 is showing the current waveforms before and after tuning.

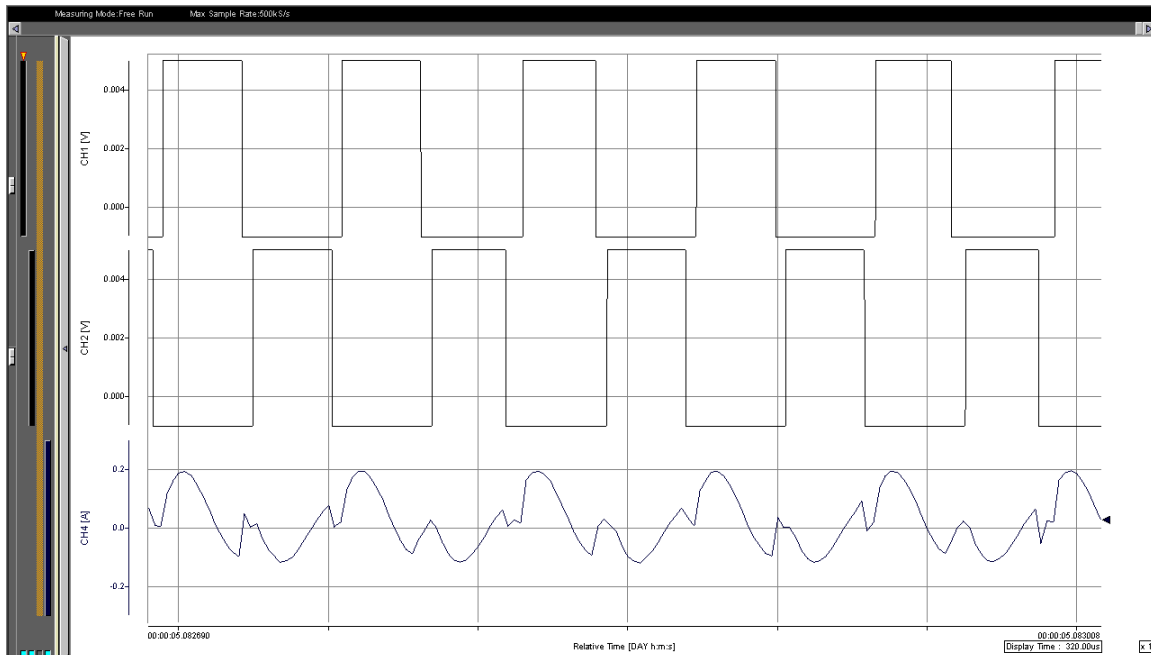


**Fig.4-4** Before tuning Waveforms

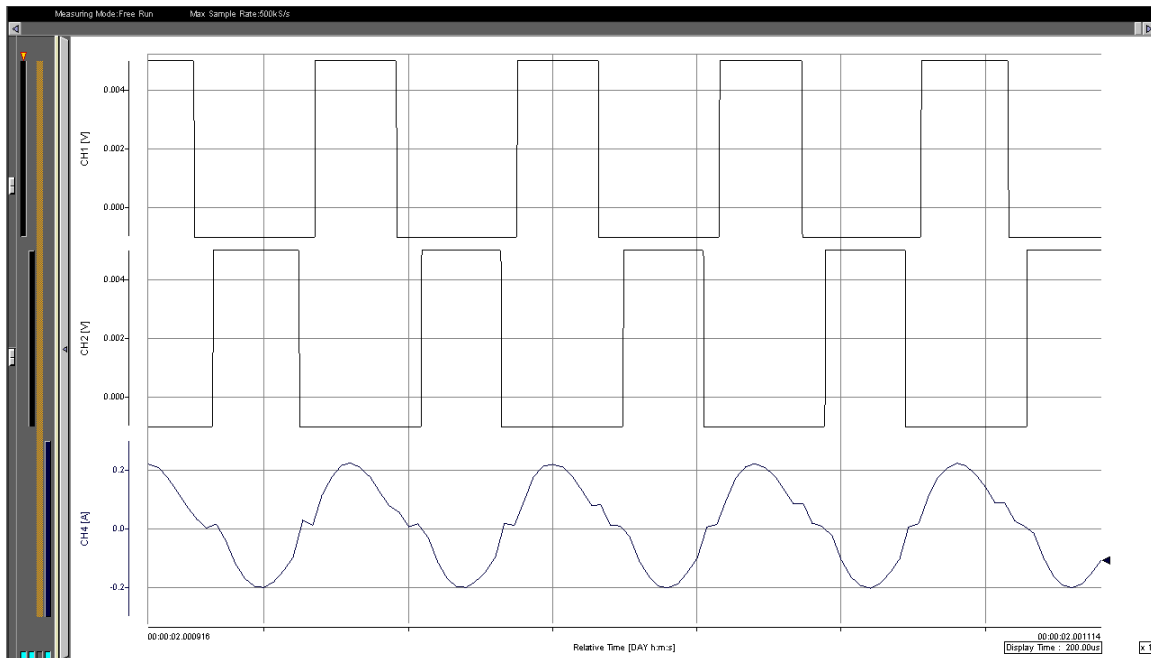


**Fig.4-5** After tuning Waveforms

The microcontroller we use have 10 bit resolution of the PWM that is mean the microcontroller cannot generate all the desired values so it is better using DSPIC with 16 bit resolution . For this reason and the tolerance of the component we may not get the exact tuning frequency. For our circuit the calculated frequency was 39215 Hz.

### **4.3 CONTROLLED SWITCHING AND EQUALIZATION TIME**

There is no direct way to measure the SoC (State of Charge ) of the battery cells but instead we can measure OCV(Open Circuit Voltage ) which is an indication of the SoC [29], the simple way for measuring the OCV is to disconnect the battery cell for at least 20 min to rest and pass the transit period and then measuring the voltage of the battery

cell, there is lot of algorithms to measure and predict the OCV and the SoC in faster way but this is beyond the scope of this thesis.

The cell B2 was discharged until its OCV reached 3.68 V and B1 is charged until its OCV reached 3.78 V and B3 is charged until OCV reached 3.75 V.

Fig.4-6 and Fig.4-7 shows charging current for B2 for SRSCC conventional method and current sharing method and how the equalization current is charging the battery in both state A and B of the circuit in current sharing method. As expected the test results must have some noise but the behaviour was the same was expected by the simulation.

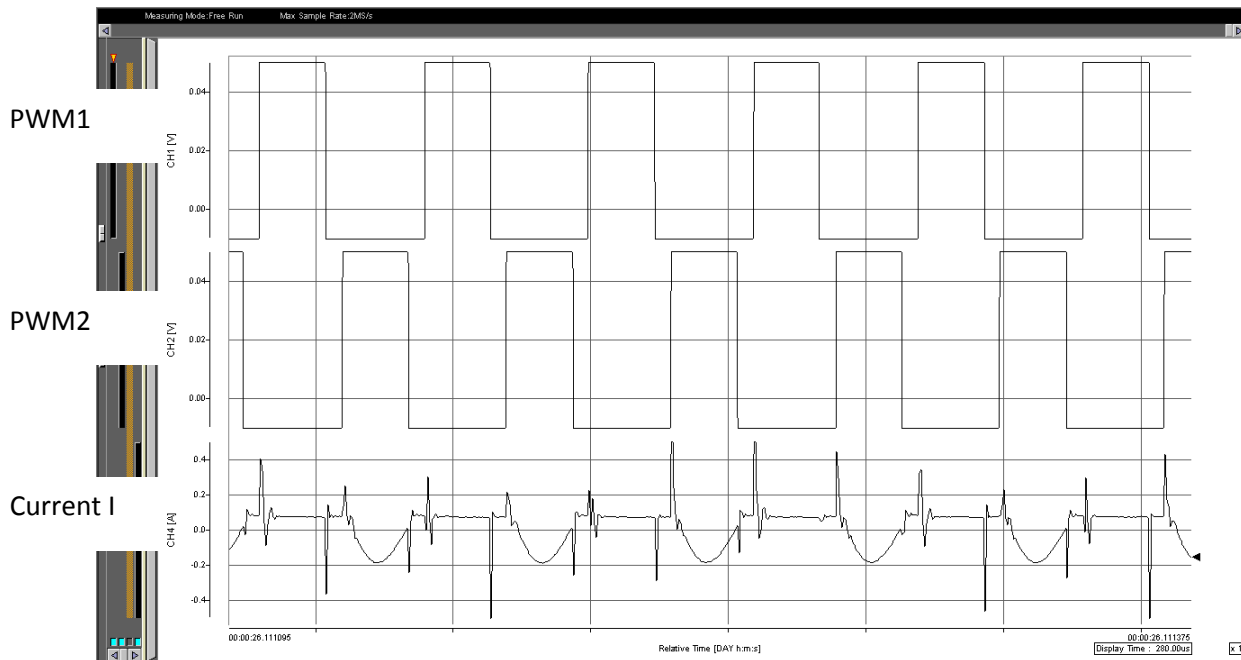


**Fig.4-6** Equalization current of B2 in SRSCC conventional method

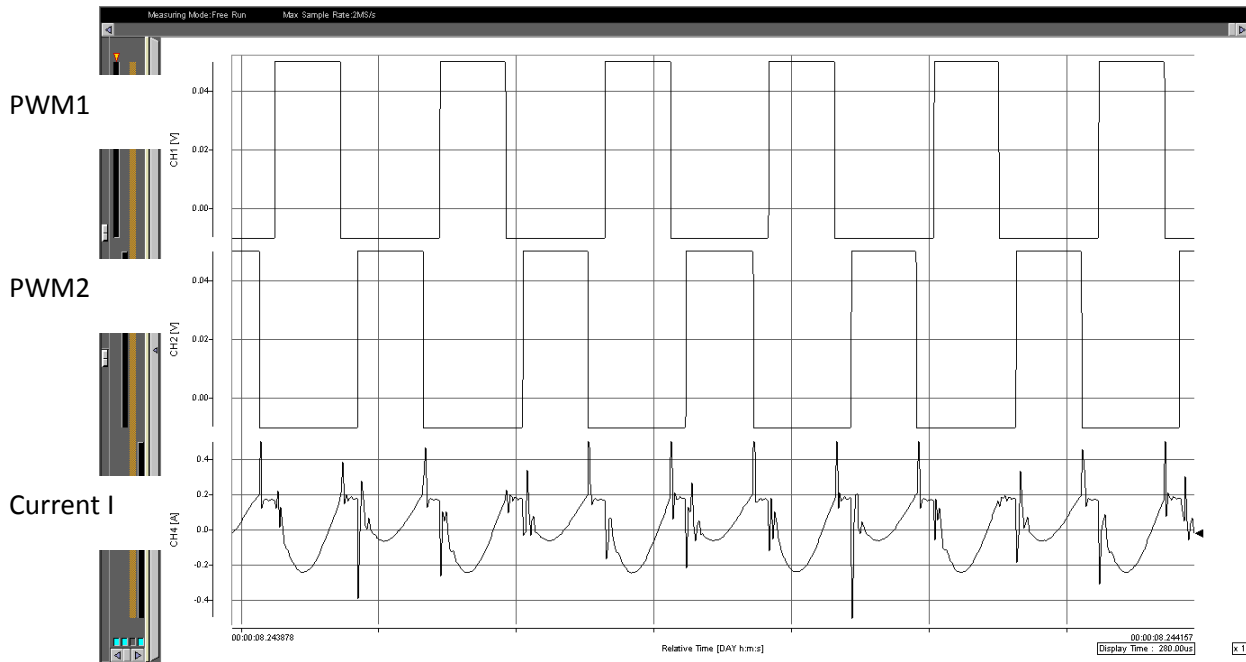


**Fig.4-7** Equalization current going to B2 in current sharing method

The zero current in Fig4-7 is the dead-band between the two PWM to avoid Shoot-through.

The measured values of the OCV for the two methods has drawn in excel using curve fitting are shown in Fig.4-8 and Fig.4-9

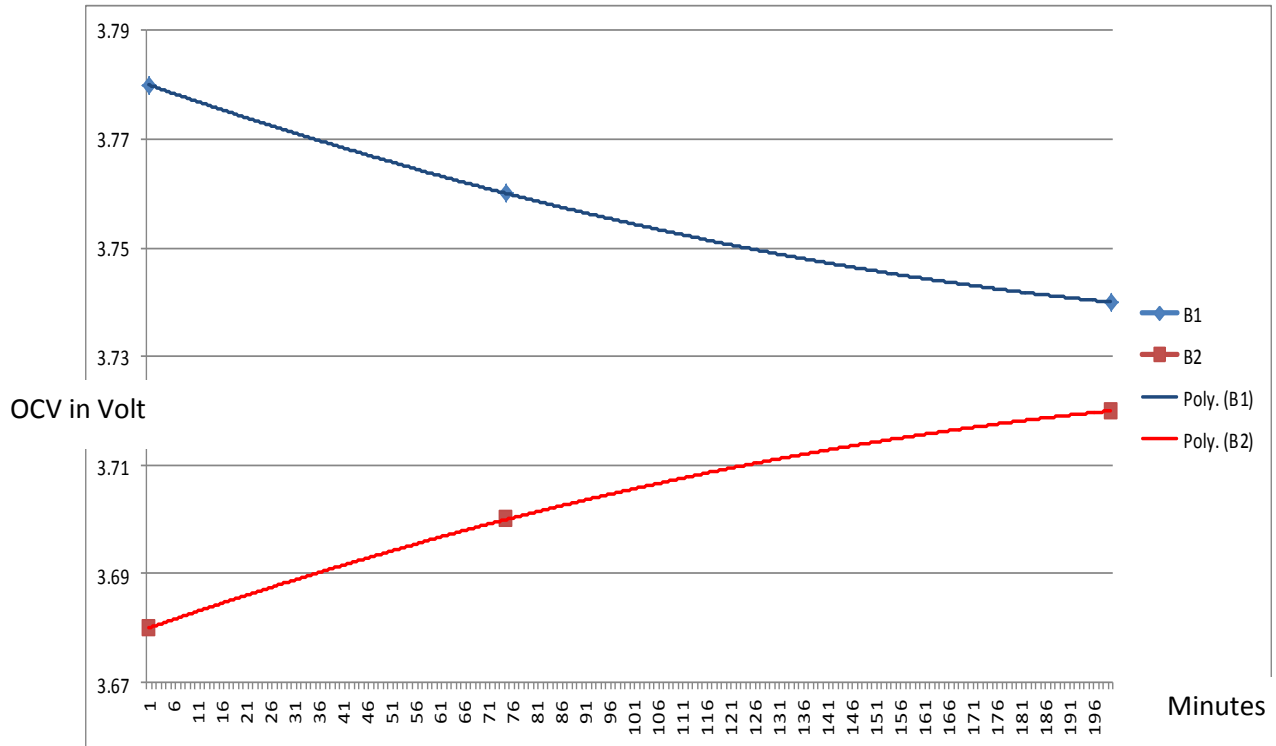


**Fig.4-8** The equalization time for two battery cell in SRSCC conventional method time in minutes



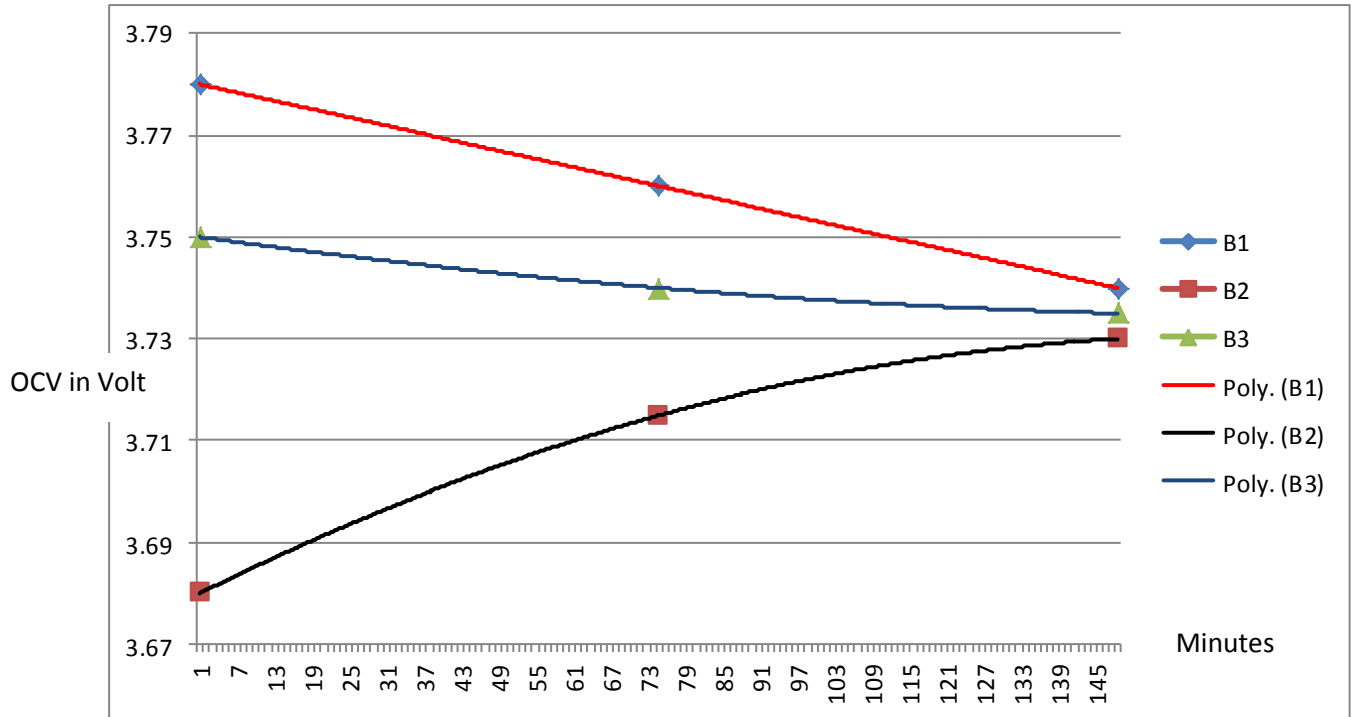


**Fig.4-9** The equalization time for three battery cell in current sharing method ( in minutes)

From Fig.4-8 It can be noticed in about 200 minute the two cells reached a voltage deference of 20mV starting from 100mV which considered fast compared to other capacitor Switching topologies.

And from Fig.4-9 it can be noticed that 10mV difference is achieved in about 148 minute and it took about 100 minute for B2 to reach 3.72 V which about the half time it took in the convention method in Fig.4-8.

## **4.4 Summary**

The prototype for four battery cells was built and the role of the microcontroller in the tuning was explained and how with the ability to select which MOSFETs can be enabled in the switching process allow the use of the current sharing method which equalize the battery in both states of the circuit state A and B .

Equalization time for the both methods conventional and current sharing was measured and showed how current sharing method enhance the circuit function and reduce the equalization time significantly.

# CHAPTER 5

## CONCLUSIONS AND FUTURE WORK

### 5.1 SUMMARY

The lifetime of the Electric Vehicle EV depends on the lifetime of its battery system, so any prolonging in the lifetime of the lithium-ion battery cells will reflect on the economic feasibility of the vehicle.

Battery cell equalization will reduce the effect of the degradation of the capacity of the cells with the time by transferring the charge from the cells with higher charge (because of the degradation of the capacity the cells will charge faster) to the other cells to prevent the discontinuity of the charging current due to reaching the maximum safe operation limit, and allowing all the cells to be charged to its maximum capacity, and as a result will prolong the lifetime of the cells.

A review of switching converter topologies for battery cell equalization was made, presenting the use of CuK converter, Buck-Boost converter, fly-back converter and Switched Capacitance converter.

Considering the SRSCC topology for the equalization is the goal of this thesis, this topology was chosen over the conventional SCC because of its benefits in soft-switching which allow the zero current switching and as result reduce the switching losses allowing higher switching frequencies, and was preferred over the inductance based converters because it needs a small inductance value just to prevent the capacitor current from

sudden changes and with small inductance value The EMI is reduced and the Weight of the equalization board is also reduced .

In chapter 3 the prove that the SRSCC topology is able to solve the equalization problem was made through the simulation and modeling. Also there was explanation of the mode of operation of the circuit for both the conventional method and the proposed current sharing method which was allowed because of the use of controlled switching.

The newly proposed Controlled switching is the ability of the microcontroller to choose and enable the MOSFETs that participate in the equalization based on the cells value and instead of transferring the charge from one cell to the adjacent cell the controlled switching is allowing the transfer of the charge from the two adjacent cells, in other words there is not only charging state and discharging state instead there will be charging and discharging simultaneously in each state and the current path will be shared for both operations that is why it has been called current sharing method, which allow a significant decrease in the equalization time between the cells

And to support the result of the simulation, a prototype board for four battery cells was built, and the key factor for choosing the component is there resistance (MOSFET with low RDS-ON , Capacitance with low ESR and Inductance with low DC resistance) and the test results was recorded in chapter 4, and it has been shown that the simulation results and the experimental results was very similar .

Also in chapter 4 the newly proposed tuning technique was explained. Since the Resonance Frequency  $f_r$  can be different from the designed Switching Frequency  $f_{sw}$  because of the tolerance of the components or the added capacitance between the tracks

or any other reason so the tuning is importance to match the Switching Frequency with the Resonance Frequency. The tuning technique was based on calculating the width of the pulse resulted from the comparator of the current signal with reference voltage to get only the positive part of the current signal. The Resonance Frequency can be calculated from equation (4-1).

But the tuning process has its limitations:

- Assuming identical component so the calculated resonance frequency is the same for other equalizing circuit because of the use of only one current sensor , and here point of interest from the sensor is not the value of the current but frequency
- The starting frequency must be lower than the resonance frequency in order the tuning to work
- PWM resolution is 10 bit (not all the desired frequency can be generated solution using dspic with high crystal frequency)

Although the proposed tuning technique can be used only with resonance circuits, the proposed controlled switching technique which allows the use of current sharing method can be used also with conventional SCC to reduce the equalization time which considered relatively high compared to the inductance based converters.

The main issue in choosing the type of equalization is the cost and by using SRSCC the cost is less than the inductive based type converter, even with the modification of using the microcontroller has no added cost because we are using the same microcontroller of

the BMS. I expect the cost for mass production for the equalizer will not exceed 10% of the battery cost which is within the acceptable range.

## 5.2 FUTURE WORK

Long equalization time relatively to the inductance based converter is the only disadvantage of this topology. So the goal of any future work should be based on reducing that time, one way could be by designing a circuit with high switching frequency (more than 100KHZ) and with component with lower resistance.

Also a potential feature is building an industrial grade and compact board by using *QFN* (*quad-flat no-leads*) pins DSP Microcontroller instead of DIP and more compact inductance and capacitance.

The limitation for reducing the equalization time is the value of Total Resistance so any reduce in resistance of the component will reduce the equalization time specially the  $R_{ds-on}$  of the MOSFETs , inductance DC resistance and ESR of the capacitor.

And also bypassing the limitation of tuning to get the exact resonance frequency will result in get the maximum equalization current.

## REFERENCES

- [1] Y. S. Lee and M. W. Cheng, "Intelligent control battery equalization for series connected lithium-ion battery strings," *IEEE Trans. on Industrial Electronics*, vol. 52, no. 5, pp. 1297-1307, Oct. 2005.
- [2] C. H. Kim, M. Y. Kim, J. H. Kim, and G. W. Moon, "Modularized charge equalizer with intelligent switch block for lithium-ion batteries in an HEV," in Proc. *31<sup>st</sup> IEEE Telecommunications Energy Conf.*, Vienna, Austria, Oct. 2009, pp.1-6.
- [3] S. Moore and P. Schneider, "A review of cell equalization methods for lithium ion and lithium Polymer battery systems," *SAE Technical Paper Series*, 2001-01-0959, pp. 1-5, March 2001.
- [4] V. Pop, H. J. Bergveld, D. Danilov, P. P. L. Regtien, and P. H. L. Notten, *Battery Management Systems: Accurate State-of-Charge Indication for Battery-Powered Applications*, Springer Science 2008.
- [5] O. Tremblay and L. A. Dessaint, "Experimental validation of a battery dynamic model for EV applications," *World Electric Vehicle Journal*, vol. 3, pp. 2032-6653, May 2009.
- [6] P. A. Cassani and S. S. Williamson, "Design, testing, and validation of a simplified control scheme for a novel plug-in hybrid electric vehicle battery cell equalizer," *IEEE Trans. on Industrial Electronics*, vol. 57, no. 12, pp. 3956-3962, Dec. 2010.
- [7] H. S. Kim, K. B. Park, S. H. Park, G. W. Moon, and M. J. Youn, "A new two-switch flyback battery equalizer with low voltage stress on the switches," in Proc. *IEEE Energy Conversion Congress and Expo.*, San Jose, CA, Sept. 2009, pp. 511-516.

- [8] Iqbal Husain, *Electric and Hybrid Vehicles: Design Fundamentals*, CRC Press, 2010.
- [9] Y. S. Lee and G. T. Cheng, "Quasi-resonant zero-current-switching bidirectional converter for battery equalization applications," *IEEE Trans. on Power Electronics*, vol. 21, no. 5, pp. 1213-1224, Sept. 2006.
- [10] Y. S. Lee, C. Y. Duh, G. T. Chen, and S. C. Yang, "Battery equalization using bidirectional Cuk converter in DCVM operation," in Proc. *36th IEEE Power Electronics Specialists Conf.*, Recife, Brazil, June 2005, pp. 765-771.
- [11] H. S. Park, C. E. Kim, C. H. Kim, G. W. Moon, and J. H. Lee, "A modularized charge equalizer for an HEV lithium-ion battery string," *IEEE Trans. on Industrial Electronics*, vol. 56, no. 5, pp. 1464-1476, May 2009.
- [12] G. X. Dong, Y. S. Yan, Y. Wei, and H. Jun, "Analysis on equalization circuit topology and system architecture for series-connected ultra-capacitor," in Proc. *IEEE Vehicle Power and Propulsion Conf.*, Harbin, China, Sept. 2008, pp. 1-5.
- [13] X. Wang, S. Yang, N. J. Park, K. J. Lee, and D. S. Hyun, "A three-port bidirectional modular circuit for Li-Ion battery strings charge/discharge equalization applications," in Proc. *IEEE Power Electronics Specialists Conf.*, Rhodes, Greece, June 2008, pp. 4695-4698.
- [14] J. W. Kimball, B. T. Kuhn, and P. T. Krein, "Increased performance of battery packs by active equalization," in Proc. *IEEE Vehicle Power and Propulsion Conf.*, Sept. 2007, Arlington, TX, pp. 323-327.



- [15] K. B. Park, H. S. Kim, G. W. Moon, and M. J. Youn, "Single-magnetic cell-to-cell charge equalization converter with reduced number of transformer windings," *IEEE Trans. on Power Electronics*, vol. 27, no. 6, pp. 2900-2911, June 2012.
- [16] H. Sakamoto, K. Murata, K. Nishijima, K. Harada, S. Taniguchi, K. Yamasaki, and G. Ariyoshi, "Balanced charging of series connected battery cells," in Proc. *IEEE 20<sup>th</sup> International Telecommunications Energy Conf.*, San Francisco, CA, Oct. 1998, pp. 311-315.
- [17] P. A. Cassani and S. S. Williamson, "Significance of battery cell equalization and monitoring for practical commercialization of plug-in hybrid electric vehicles," in Proc. *IEEE Applied Power Electronics Conf. and Expo.*, Washington, DC, Feb. 2009, pp. 465-471.
- [18] A. C. Baughman and M. Ferdowsi, "Double-tiered switched-capacitor battery charge equalization technique," *IEEE Trans. on Industrial Electronics*, vol. 55, no. 6, pp. 2277-2285, June 2008.
- [19] C. Pascual and P. T. Krein, "Switched capacitor system for automatic series battery equalization," in Proc. *IEEE Applied Power Electronics Conf. and Expo.*, Atlanta, GA, Feb. 1997, vol. 2, pp. 848-854.
- [20] M. Chen and R. Mora, "Accurate electrical battery model capable of predicting runtime and I-V performance," *IEEE Trans. on Energy Conversion*, vol. 21, no. 2, pp. 504- 511, June 2006.
- [21] O. Tremblay, L. A. Dessaint, and A. I. Dekkiche, "A generic battery model for the dynamic simulation of hybrid electric vehicles," in Proc. *IEEE Vehicle Power and Propulsion Conf.*, Arlington, TX, Sept. 2007, pp. 284-289.

- [22] J. W. Kimball and P. T. Krein, "Analysis and design of switched capacitor converters," in Proc. *IEEE Applied Power Electronics Conf. and Expo.*, Austin, TX, March 2005, vol. 3, pp. 1473-1477.
- [23] A. Baughman and M. Ferdowsi, "Analysis of the double-tiered three-battery switched capacitor battery balancing system," in Proc. *IEEE Vehicle Power and Propulsion Conf.*, Windsor, UK, Sept. 2006, pp. 1-6.
- [24] J. Cao, N. Schofield, and A. Emadi, "Battery balancing methods: A comprehensive review," in Proc. *IEEE Vehicle Power and Propulsion Conf.*, Harbin, China, Sept. 2008, pp. 1-5.
- [25] K. W. E. Cheng, B. P. Divakar, H. Wu, K. Ding, and H. F. Ho, "Battery-management system (BMS) and SOC development for electrical vehicles," *IEEE Trans. on Vehicular Technology*, vol. 60, no. 1, pp. 76-88, Jan. 2011.
- [26] C. Speltino, A. Stefanopoulou, and G. Fiengo, "Cell equalization in battery stacks through State of Charge estimation polling," in Proc. *IEEE American Control Conf.*, Baltimore, MD, June 2010, pp. 5050-5055.
- [27] Y. S. Lee, M. W. Chen, K. L. Hsu, J. Y. Du, and C. F. Chuang, "Cell equalization scheme with energy transferring capacitance for series connected battery strings," in Proc. *IEEE Region 10 Conf. on Computers, Communications, Control and Power Engineering*, Beijing, China, Oct. 2002, vol. 3, pp. 2042- 2045.
- [28] A. Baughman and M. Ferdowsi, "Double-tiered capacitive shuttling method for balancing series-connected batteries," in Proc. *IEEE Vehicle Power and Propulsion Conf.*, Chicago, IL, Sept. 2005, pp. 109-113.

- [29] B. T. Kuhn, G.E. Pitel, and P. T. Krein, "Electrical properties and equalization of lithium-ion cells in automotive applications," in Proc. *IEEE Vehicle Power and Propulsion Conf.*, Chicago, IL, Sept. 2005, pp. 7-9.
- [30] A. Emadi, "Modeling and analysis of multiconverter DC power electronic systems using the generalized state-space averaging method," *IEEE Trans. on Industrial Electronics*, vol. 51, no. 3, pp. 661-668, June 2004.
- [31] J. W. Kimball, P. T. Krein, and K. R. Cahill, "Modeling of capacitor impedance in switching converters," *IEEE Power Electronics Letters*, vol. 3, no. 4, pp. 136-140, Dec. 2005.
- [32] M. Shoyama, F. Deriha, and T. Ninomiya, "Operation, analysis and control of resonant boost switched capacitor converter with high efficiency," in Proc. *IEEE Power Electronics Specialists Conf.*, Recife, Brazil, June 2005, pp. 1966-1971.
- [33] A. Shafiei and S. S. Williamson, "Plug-in hybrid electric vehicle charging: current issues and future challenges," in Proc. *IEEE Vehicle Power and Propulsion Conf.*, Lille, France, Sept. 2010, pp. 1-8.
- [34] Y. Lee and Y. P. Ko, "Switched-capacitor bi-directional converter performance comparison with and without quasi-resonant zero-current switching," *IET Power Electronics*, vol. 3, no. 2, pp. 269-278, March 2010.
- [35] G. A. Kobzev, "Switched-capacitor systems for battery equalization," in Proc. *IEEE 6<sup>th</sup> International Scientific and Practical Conf. of Students, Post-graduates and Young Scientists, Modern Techniques and Technology*, Tomsk, Russia, March 2000, pp. 57-59.

- [36] X. Wei and B. Zhu, "The research of vehicle power Li-ion battery pack balancing method," in Proc. *IEEE International Conf. on Electronic Measurement and Instruments*, Beijing, China, Aug. 2009, vol. 2, pp. 498-502.
- [37] Y. S. Lee and S. C. Chu, "EMI performance comparison of switched-capacitor bidirectional converter with and without QR ZCS," in Proc. *IEEE International Conf. on Power Electronics and Drive Systems*, Taipei, Taiwan, Nov. 2009, pp. 1137-1142.
- [38] W. C. Lee, D. Drury, and P. Mellor, "Comparison of passive cell balancing and active cell balancing for automotive batteries," in Proc. *IEEE Vehicle Power and Propulsion Conf.*, Chicago, IL, Sept. 2011, pp. 1-7.
- [39] Y. S. Lee, Y. Y. Chiu, and M. W. Cheng, "Inverting ZCS switched-capacitor bi-directional converter," in Proc. *IEEE Power Electronics Specialists Conf.*, Jeju, South Korea, June 2006, pp. 1-6.
- [40] Y. S. Lee and Y. Y. Chiu, "Zero-current-switching switched-capacitor bidirectional DC-DC converter," *IEE Proceedings Electric Power Applications*, vol. 152, no. 6, pp. 1525- 1530, Nov. 2005.
- [41] Y. S. Lee and G. T. Chen, "ZCS bi-directional DC-to-DC converter application in battery equalization for electric vehicles," in Proc. *IEEE Power Electronics Specialists Conf.*, Aachen, Germany, June 2004, vol. 4, pp. 2766- 2772.
- [42] Z. G. Kong, C. B. Zhu, R. G. Lu, and S. K. Cheng, "Comparison and Evaluation of Charge Equalization Technique for Series Connected Batteries," in Proc. *IEEE Power Electronics Specialists Conf.*, Jeju, South Korea, June 2006, pp. 1-6.